GEOLOGICAL JOURNAL
Geol. J. **48**: 467–483 (2013)
Published online 28 January 2013 in Wiley Online Library
(wileyonlinelibrary.com). DOI: 10.1002/gj.2486

C–O isotope geochemistry of the Dashiqiao magnesite belt, North China Craton: implications for the Great Oxidation Event and ore genesis

HAO-SHU TANG [1,2], ***YAN-JING CHEN*** [2,3]*, ***M. SANTOSH*** [4,5], ***HONG ZHONG*** [1], ***GUANG WU*** [3] and ***YONG LAI*** [2]

[1] *State Key Laboratory of Ore Deposit Geochemistry, Institute of Geochemistry, Chinese Academy of Sciences, Guiyang, China*
[2] *Key Laboratory of Crustal and Orogenic Evolution, Peking University, Beijing, China*
[3] *Key Laboratory of Mineralogy and Metallogeny, Guangzhou Institute of Geochemistry, Chinese Academy of Sciences, Guangzhou, China*
[4] *Division of Interdisciplinary Science, Faculty of Science, Kochi University, Kochi, Japan*
[5] *Journal Center, China University of Geosciences, Beijing, China*

The worldwide 2.33−2.06 Ga unique positive $\delta^{13}C_{carb}$ excursion has been correlated with the Great Oxidation Event (GOE). The Dashiqiao Formation in the Liaohe Group of the northeastern North China Craton formed at 2.2−2.174 Ga and hosts one of the world-class magnesite deposits. Here we present major element and C and O isotope analyses of 22 samples from the Dashiqiao Formation and use the data to evaluate the impact of the GOE in the North China Craton, as well as the genesis of the Dashiqiao giant magnesite deposits. Six dolomitic marble samples from a ~600 m thick interval with 1.10 ± 0.04 of MgO/CaO (mol) ratios show higher $\delta^{13}C_{PDB}$ values of 0.6−1.4‰ (average 1.2 ± 0.3‰) than those of normal marine carbonates over the globe. However, they display lower $\delta^{18}O_{SMOW}$ of 16.4−19.5‰ (average 18.2 ± 1.1‰) as compared to their contemporaneous counterparts, suggesting that the primary carbonates in the Dashiqiao Formation should possess a positive $\delta^{13}C$ anomaly (possibly 4.2‰) reflecting the impact of the GOE, and that the $\delta^{13}C$ and $\delta^{18}O$ values have been depleted in post-sedimentation diagenesis and/or regional metamorphism. The >550 m thick magnesite layer in the studied section has MgO/CaO ratios ranging from 4.45−200.00. These rocks show $\delta^{13}C$ and $\delta^{18}O$ values of 0.1−0.9‰ and 9.2−16.9‰, with average values of 0.4 ± 0.2‰ and 13.3 ± 2.5‰, respectively, obviously lower than those of the underlying dolomites. The depletions of ^{13}C and ^{18}O in magnesites relative to dolomitic marbles are interpreted to be the result of hydrothermal alteration related to regional metamorphism leading to rock recrystallization and mass exchange. This interpretation is further confirmed from the hanging-wall dolomitic marble and the veinlet-filled magnesite from the ore layer. The former contains mega-crystals of cylindrical talc and has $\delta^{13}C$ of −2.6‰ and $\delta^{18}O$ of 14.1‰, indicating that a local fluid–rock interaction between (argillaceous) dolomite and (siliceous) hydrothermal fluids poor in ^{13}C and ^{18}O resulted in the formation of talc and further depletion both in $\delta^{13}C$ and in $\delta^{18}O$. The veinlet-filled magnesite yields $\delta^{13}C$ and $\delta^{18}O$ values of −2.7‰ and 16.2‰, respectively, showing lower $\delta^{13}C$ but higher $\delta^{18}O$ than those of massive magnesite in the adjacent strata. Our observation thus strongly supports the interpretation that the massive magnesite interacted with low-$\delta^{13}C$ fluids which were possibly sourced from meteoric water at low temperature during post-ore time. Thus, the formation of the Dashiqiao magnesite deposits involved primary sedimentation, diagenesis, regional metamorphism, hydrothermal replacement and local post-ore fluid–rock interaction. Copyright © 2013 John Wiley & Sons, Ltd.

Received 22 April 2012; accepted 13 December 2012

KEY WORDS Great Oxidation Event (GOE); Dashiqiao magnesite belt; Liaohe Group; C−O isotopes; petrogenesis; North China Craton

1. INTRODUCTION

The Archaean/Proterozoic transition in Earth history witnessed dramatic changes, which include the formation of numerous cratonic basins in the Proterozoic as against the widespread greenstone belts in the Archaean. From the dawn of the Proterozoic, voluminous red beds, evaporites, stromatolite-bearing carbonates (Chen, 1990; Melezhik *et al*., 1999; Tang *et al*., 2009, 2011), Superior-type banded iron formations (Huston and Logan, 2004; and references therein), phosphate, and rare earth element deposits (Tu *et al*., 1985; Chen, 1990; Zhao, 2010, and references therein), and magnesite deposits (e.g. the Dashiqiao magnesite belt deposits; Chen and Cai, 2000; Chen *et al*., 2003a, b; Jiang *et al*., 2004) evolved rapidly. The tectonic processes and global environmental change during the Palaeoproterozoic from 2.5 to 1.6 Ga have been the focus of numerous studies in the past. Schidlowski *et al*. (1975, 1976) first discovered

*Correspondence to: Y.-J. Chen, Key Laboratory of Crustal and Orogenic Evolution, Peking University, Beijing 100871, China. E-mail: yjchen@pku.edu.cn

the positive $\delta^{13}C_{carb}$ anomaly in the ~2.0 Ga carbonates from Karelia (Russia) and the Fennoscandian shields, and also in the dolomites with ages of 2.65–1.95 Ga from the Lomagundi Province (Zimbabwe). They also related this phenomenon to the oxidation of the atmosphere. However, this important discovery had been largely neglected until 1990.

In 1989, the International Commission on Stratigraphy recommended 2.3 Ga as the boundary between the Siderian and the Rhyacian in the Precambrian Stratigraphy Chart. Thereafter, more attention was focused on the nature of the 2.3 Ga stratigraphic boundary (Chen, 1988, 1990; Chen and Fu, 1992; Chen and Su, 1998) and several workers recognized marked positive $\delta^{13}C$ excursions in the worldwide 2.33–2.06 Ga carbonate strata (Schidlowski, 1988; Bekker *et al.*, 2003a, b, 2006; Tang *et al.*, 2011, 2012, and references therein). The positive $\delta^{13}C_{carb}$ excursion was variously termed as the Lomagundi Event (Karhu and Holland, 1996), the Jatulian Event (Melezhik and Fallick, 1996; Melezhik *et al.*, 1999) or the Great Oxidation Event (GOE) (Anbar *et al.*, 2007; Konhauser *et al.*, 2009; Zhao, 2010) and was genetically correlated to global environmental changes (Karhu and Holland, 1996; Melezhik *et al.*, 1999; Chen *et al.*, 2000; Young, 2012a, b), to the breakup of the Kenorland/Superia supercontinent (Bekker and Eriksson, 2003), or to a 2.3 Ga environmental catastrophe, as indicated by the contrasting rare earth element geochemical signatures between pre- and post-2.3 Ga sediments (Chen, 1988, 1990; Chen *et al.*, 1994, 1998; Chen and Zhao, 1997; Tang *et al.*, 2012). Melezhik *et al.* (1999) suggested that the Lomagundi Event consists of several sub-events, whereas Bekker *et al.* (2003a) considered that it is a single long-lasting event. The recognition of the GOE or environmental catastrophe was one of the most important progresses in the research on the Precambrian, and provided insights into our understanding of the Precambrian evolution and mineralization during the early Earth history.

The North China Craton (NCC; Fig. 1) is an Early Precambrian continental block with widespread Palaeoproterozoic strata (see Zhai *et al.*, 2010; Zhai and Santosh, 2011; Zheng *et al.*, 2012), including the Liaohe Group in the Jiao-Liao-Ji Belt (Fig. 2), which hosts one of the largest magnesite ore belts of the world (the Dashiqiao magnesite belt; Fig. 3), together with numerous other ore deposits (Zhang *et al.*, 1988; Peng and Palmer, 1995; Jiang *et al.*, 1997, 2004; Wang *et al.*, 1998; Chen and Cai, 2000; Peng, 2002; Xiao *et al.*, 2003; Wang and Peng, 2008), such as the Houxianyu B, Qingchengzi Pb–Zn and Lianshanguan U ores. However, several questions remain unanswered including

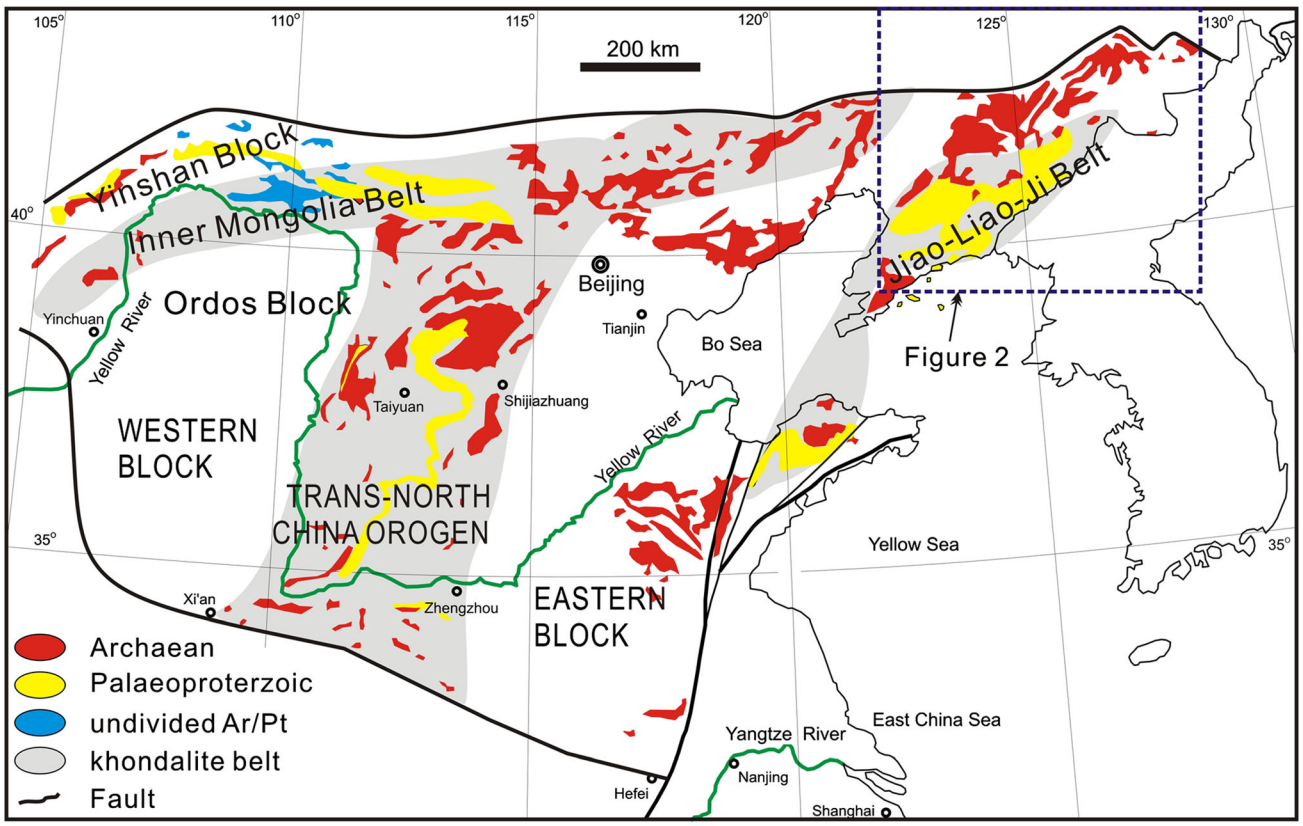

Figure 1. Archaean–Palaeoproterozoic terranes of the North China Craton (modified after Zhai *et al.*, 2010). Ar/Pt = Archaean/Proterozoic. This figure is available in colour online at wileyonlinelibrary.com/journal/gj

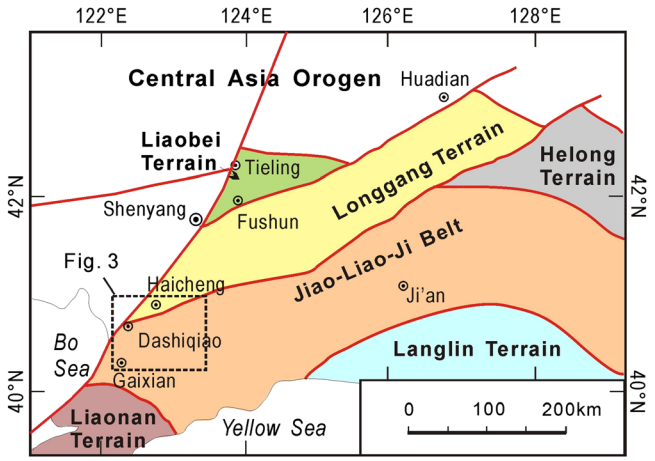

Figure 2. Tectonic framework of the northeast part of the North China Craton (cited from Tang *et al*., 2012). See Figure 1 for location. This figure is available in colour online at wileyonlinelibrary.com/journal/gj

whether these Palaeoproterozoic strata record the GOE or Lomagundi Event, and whether the sedimentary–metamorphic deposits are genetically related to the GOE (Tang *et al*., 2009; Zhai *et al*., 2010). A key to these problems is important in understanding the Precambrian evolution and mineralizations of the North China Craton. In this study, therefore, we carried out geological and geochemical investigations on the giant Dashiqiao magnesite deposits and its host-rocks within the Liaohe Group. We report new geochemical data for the Dashiqiao Formation, and evaluate the problems related to the GOE, and the implications of the mineralization in the North China Craton.

2. GEOLOGY AND STRATIGRAPHY

Recent models propose that the Precambrian crustal evolution history of the North China Craton involved three main phases: (1) a major phase of continental growth at *ca*. 2.7 Ga; (2) the amalgamation of micro-blocks and cratonization at *ca*. 2.5 Ga; and (3) Palaeoproterozoic rifting–subduction–accretion–collision tectonics and subsequent high-grade granulite facies metamorphism–granitic magmatism during *ca*. 2.0–1.82 Ga (Diwu *et al*., 2011; Liu *et al*., 2011; Tsunogase *et al*., 2011; Wan *et al*., 2011; Zhai and Santosh, 2011; Liu *et al*., 2012; Santosh *et al*., 2012). The Precambrian basement of the North China Craton can be divided into the Eastern and Western blocks dissected by three major Palaeoproterozoic accretionary belts, namely, the Khondalite Belt or the Inner Mongolia Belt, the Trans-North China Orogen and the Jiao-Liao-Ji Belt (Fig. 1; Zhao *et al*., 2005; Zhai *et al*., 2010; Kusky, 2011; Santosh *et al*., 2012; Zheng *et al*., 2012). The roughly E−W-trending Khondalite Belt or the Inner Mongolia Suture Zone is interpreted as a Palaeoproterozoic collisional belt along which the Yinshan and Ordos blocks amalgamated to form the Western Block (Santosh, 2010; Santosh *et al*., 2012, and references therein), which then collided with the Eastern Block along the Trans-North China Orogen to form the basement of the North China Craton (Fig. 1; Zhao *et al*., 2005; Zhai *et al*., 2010; Kusky, 2011). The Jiao-Liao-Ji Belt is located within the Eastern Block and its tectonic setting and nature remain controversial; some invoking the opening and closing of a Palaeoproterozoic intra-continental rift (Li and Zhao, 2007; Zhai and Peng, 2007; Luo *et al*., 2008), whereas others suggesting the development of an island arc and its collision with continental blocks in the Palaeoproterozoic (Zhang *et al*., 1988; He and Ye, 1998; Faure *et al*., 2004), or as a major Palaeoproterozoic collisional suture (Tam *et al*., 2012).

The northeast part of the North China Craton includes the Liaobei, Longgang and Helong terrains in the north, the Liaonan and Langlin terrains in the south, with the Jiao-Liao-Ji Belt in the middle (Fig. 2). These terrains (or belts) comprise Archaean granite–greenstone associations and Palaeoproterozoic lithostratigraphic successions (Zhang *et al*., 1988; Sun *et al*., 1993; Zhao *et al*., 2004, 2005; Wan *et al*., 2006; Li and Zhao, 2007; Tam *et al*., 2011). The Jiao-Liao-Ji Belt, however, is mainly composed of Palaeoproterozoic sedimentary and volcanic successions that are metamorphosed in the greenschist to lower amphibolite facies and tectonically associated with granitic and mafic intrusions (Li *et al*., 2006). Recent studies have reported high pressure pelitic granulites from this belt, suggesting a continental collision zone (Tam *et al*., 2012).

The Palaeoproterozoic Liaohe Group is best developed in the Jiao-Liao-Ji Belt (Fig. 3) and unconformably overlies the Archaean Anshan Group (Liaoning Bureau of Geology and Mineral Resources, 1989). The stratigraphy of the Liaohe Group in the Jiao-Liao-Ji Belt shows a progression from a basal clastic-rich sequence and a lower bimodal-volcanic sequence, through a middle high-Mg carbonate-rich sequence, to an upper pelite-rich sequence (Wan *et al*., 2006; Luo *et al*., 2008), and includes, in ascending order, the Langzishan, Lieryu, Gaojiayu, Dashiqiao and Gaixian formations (Fig. 4). The Langzishan Formation is 244–1278 m thick and comprises graphite-bearing calc feldspar-quartz schist, amphibolite, sillimanite-bearing mica schist and thin-bedded marbles, with conglomerate or quartzite at the base. The Lieryu Formation is ~976 m thick and well known for borate deposits, such as the Houxianyu szaibelyite deposit (Jiang *et al*., 1997) and the Wengquangou ludwigite deposit (Wang and Peng, 2008), which are hosted in schists and dolomitic marbles. Its protolith is thought to include felsic–intermediate lava, pyroclastic rocks, tuffs, sandstones and carbonate rocks. The Gaojiayu Formation is 371−557 m thick and consists of garnet-bearing two-mica quartz schist, biotite schist, phyllite and dolomitic marble. The Dashiqiao Formation is well known for its talc, magnesite and serpentine deposits (Chen *et al*., 2003a, b; Jiang

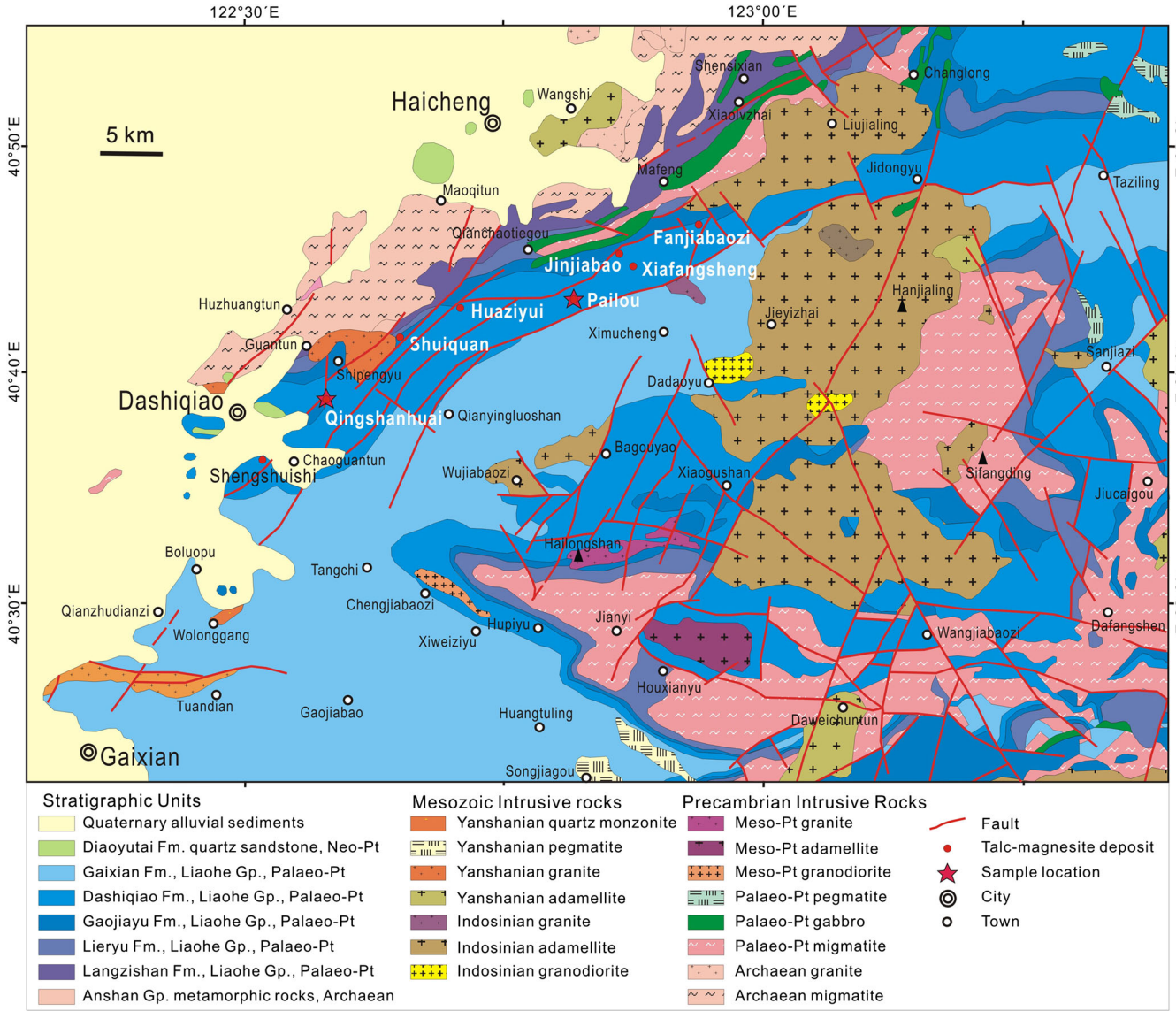

Figure 3. Simplified geological map showing distribution of the Liaohe Group in the Dashiqiao magnesite belt and positions of the Qingshanhuai and Pailou magnesite deposits (modified after Liaoning Bureau of Geology and Mineral Resources, 1989, and Jiang *et al*., 2004). See Figure 2 for location.

et al., 2004) that are hosted in a 1054–3890 m thick carbonate–slate–phyllite–schist succession predominated by dolomitic marble. The Gaixian Formation is widely developed with a fairly uniform thickness of *ca*. 2415 m and a lithologic association of two-mica schist, mica-bearing feldspathic schist, quartzite, phyllite and slate.

Detrital zircons in biotite–plagioclase gneiss from the Langzishan Formation have yielded concordant SHRIMP U–Pb ages of ~2.2 and ~2.4 Ga, respectively, whereas metamorphic zircon gave a SHRIMP U–Pb upper intercept age of *ca*. 1.86 Ga, which was interpreted to record the 1.85 Ga metamorphic event (Wan *et al*., 2006). Detrital zircons with magmatic features from the Langzishan Formation have yielded concordant LA-ICP-MS U–Pb ages from 2.05 to 2.24 Ga (Luo *et al*., 2004). The SHRIMP U–Pb age for igneous zircons from fine-grained biotite gneiss of the Lieryu Formation is *ca*. 2.18 Ga (Wan *et al*., 2006), and near-concordia SHRIMP U–Pb ages for detrital zircons in quartzite of the Gaixian Formation fall in the range of 2.22–2.02 Ga (Wan *et al*., 2006). All these ages suggest that the Liaohe Group was deposited in the interval 2.24–2.02 Ga, and metamorphosed at about 1.86 Ga. This conclusion is supported by the age data on the Liaoji granite complex which intruded the lower portion of Liaohe Group and is considered to have developed somewhat coevally with the Liaohe Group (Zhang *et al*., 1988). For example, a tourmaline-

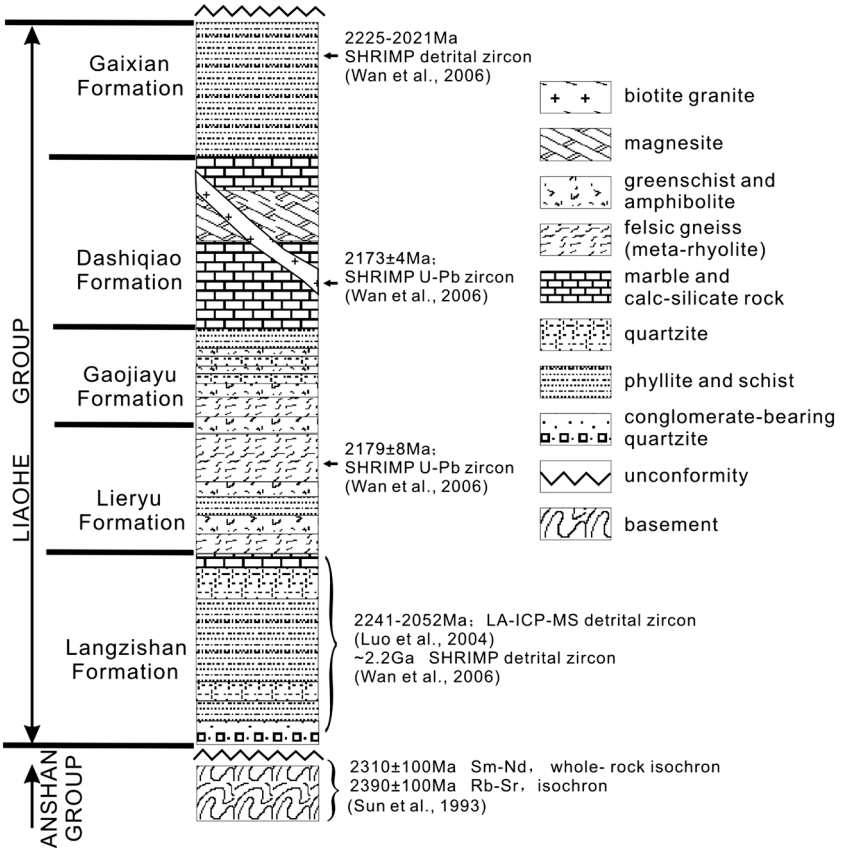

Figure 4. The stratigraphic units of the Liaohe Group in the Jiao-Liao-Ji Belt (modified after Li *et al*., 2005).

bearing muscovite monzogranite in the Hupiyu area intruding the lower portion of the Liaohe Group has yielded LA-ICP-MS zircon U–Pb age of 2163 ± 15 Ma (Lu *et al*., 2004); similar intrusions in the Fengcheng area have yielded SHRIMP zircon U–Pb ages of 2168 ± 13 and 2094 ± 6 Ma, respectively (Li *et al*., 2005). The granites in the Tonghua area record SHRIMP zircon U–Pb ages of 2158 ± 13, 2164 ± 8 and 2147 ± 12 Ma (Lu *et al*., 2006), and the Pailou biotite granite in the Dashiqiao area has yielded a concordant SHRIMP zircon U–Pb age of 2173 ± 4 Ma (Wan *et al*., 2006). The zircon U–Pb ages from the granitoids range from 2173 ± 4 to 2094 ± 6 Ma and in the 2.24–2.02 Ga interval is inferred to mark the timing of deposition of the Liaohe Group.

The northwestern part of the Jiao-Liao-Ji Belt is famous for hosting world-class magnesite, talc and borate deposits. A number of important magnesite deposits, including the Shengshuishi, Qingshanhuai, Shuiquan, Huaziyu, Pailou, Jinjiabao, Xiafangsheng and Fanjiabaozi deposits (Fig. 3), occur in the Dashiqiao magnesite belt (Fig. 3), and are mainly located in the Haicheng and Dashiqiao counties, Liaoning Province. These deposits are controlled by the third member of the Dashiqiao Formation with bedded or lens-type occurrence, and comprise an important part of the Dashiqiao strata. The proven reserve of magnesite in this belt is 2.987 billion tons (The Ministry of Land and Resources of China, 2001), accounting for >80% of the total magnesite reserves in China and up to 30% of the world reserves (Chen *et al*., 2003a). The Dashiqiao magnesite belt has been an important topic for the IGCP443 (International Geology and Environment Comparison of Magnesite and Talc) project (Chen *et al*., 2003b; Jiang *et al*., 2004).

3. SAMPLES AND ANALYTIC METHODS

Samples in this study were collected from the Qingshanhuai (Fig. 5A) and Pailou (Fig. 5B) mining areas. A geological profile survey has been conducted in the Qingshanhuai area, starting from the hanging-wall dolomitic marble (122°35.554′E, 40°38.848′N), continuing northward across the magnesite deposit, and culminating at the footwall rocks (122°34.623′E, 40°39.137′N). The thickness of magnesite orebody in this area is up to 550 m. The orebody occurs conformably within dolomitic marbles in both the hanging and foot walls. A fault has been inferred between the orebody and hanging-wall dolomites which are heterogeneously broken and hydrothermally altered. Diabase dykes

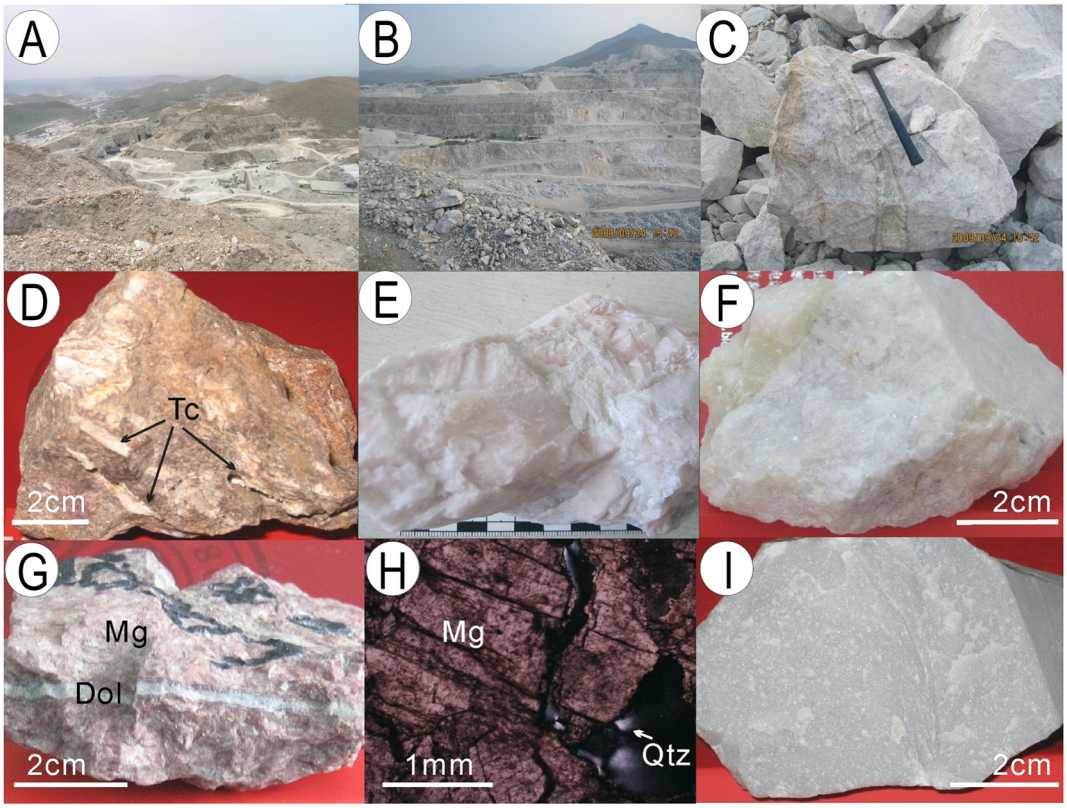

Figure 5. Geological characteristics of samples from the Qingshanhuai and Pailou magnesite deposits. (**A**) Qingshanhuai ore area. (**B**) Pailou ore area. (**C**) Coarse-grained magnesite, relict banded texture, sample HLD03. (**D**) Hanging-wall dolomitic marble with mega-cylindrical talc crystals, sample LD001. (**E**) Massive shallow pink coarse-grained magnesite, sub-equigranular texture, sample HLD02. (**F**) Massive white magnesite ore, sample LD002. (**G**) Pink, coarse-grained magnesite ore disseminated with fine-grained carbonate-quartz veinlets, sample LD006. (**H**) Micrograined quartz in veinlets, sample LD006. (**I**) The footwall dolomitic marble, sample LD011. Mineral abbreviations: Tc, talc; Dol, dolomite; Mg, magnesite; Qtz, quartz. This figure is available in colour online at wileyonlinelibrary.com/journal/gj

cutting the magnesite orebody can be also observed at the Qingshanhuai area. The Pailou samples were collected from the location with co-ordinates of 122°48.525′E, 40°43.645′N.

The details of individual samples are summarized in Table 1. Among these, the Qingshanhuai area, sample LD001 was collected from the hanging wall in direct contact with the orebody. Samples LD002−LD008 were collected from the orebody and are coarsely recrystallized magnesite rocks, locally developed as veinlets with thickness up to 5 mm. Samples LD009−LD014 come from massive microsparite dolomitic marbles in the footwall. Samples HLD01−HLD08 come from the orebody at the Pailou deposit. The samples (0.5–2 kg) were reduced in size using a steel press and a percussion mortar. Small dolostone chips (~1 mm in size, without secondary veins/minerals) were handpicked and ultrasonically cleaned in deionized water and subsequently milled in an agate mortar. Major elements were analyzed by X-ray fluorescence spectrometry at the Key Laboratory of Crust and Orogen Evolution, Peking University, China, using an ARL ADVANTXP+ X-ray spectrometer calibrated against limestone GSR13 and GSR6. The detection limit for the element is around 0.001%, and the precision (1σ) is typically <1% for the major oxide. Carbon and oxygen isotope analyses of the 14 carbonate samples were conducted at the Isotope Laboratory of the Institute of Mineral Resources, Chinese Academy of Geological Sciences, Ministry of Land and Resource of China, Beijing. Carbon and oxygen isotopic compositions of carbonates were measured on CO_2 on the MAT-253 mass spectrometer. Under vacuum, the CO_2 was liberated and collected from powdered carbonates using 100% phosphoric acid for operation at 50 ± 0.2 °C for 24 h. Then the CO_2 was collected, condensed and purified in a liquid nitrogen-alcohol cooling trap (−70 °C) for $\delta^{13}C$ mass spectrometry analysis. The $\delta^{13}C$ data are reported in per mill relative to V-PDB and the $\delta^{18}O$ data in per mill relative to V-PDB and V-SMOW, respectively. The precision (1σ) for both isotope ratios is better than ±0.2‰. Oxygen isotope data for dolomites were corrected using the fractionation factor 1.01066 (Rosenbaum and Sheppard, 1986; Chen *et al.*, 2005), and $\delta^{18}O_{V\text{-}SMOW}$ was calculated according to $\delta^{18}O_{V\text{-}SMOW} = 1.03086 \times \delta^{18}O_{PDB} + 30.86$ (Friedman and O'Neil, 1977).

Table 1. Geology of samples from the Qingshanhuai and Pailou deposits, Dashiqiao magnesite belt

No.	Sample	Stratigraphic height (m)	Lithology
Qinshanhuai			
LD001	Talc-dolomitic marble	1100	Dark-pink dolomitic marble composed of ~15% cylindrical talc with length up to 2 cm, and ~85% hypidiomorphic dolomite with size of 0.01–0.3 mm (Fig. 5D)
LD002	Magnesite	1044	Light green variegated white in colour, silicified and serpentinized, coarse-grained magnesite (Fig. 5F); from fractured zone on the top of ore-bearing strata
LD003	Magnesite	985	Straw yellow, coarse-grained, massive magnesite, nearby a diabase dyke
LD004	Magnesite	890	White, coarse sub-equigranular grained, massive magnesite
LD005	Magnesite	838	Light pink, coarse sub-equigranular grained, massive magnesite
LD006	Veinlet-filled magnesite	815	Flesh-red coarse-grained magnesite, with pale grey fine-grained carbonate veins (Fig. 5G, H)
LD007	Magnesite	735	Shallow pink, coarse-grained, massive magnesite
LD008	Magnesite	573	Shallow pink, coarse-grained, massive magnesite
LD009	Dolomitic marble	339	Grey, massive, microsparite dolomitic marble, with a few micrograined quartz veinlets
LD010	Dolomitic marble	172	Grey, massive, microsparite dolomitic marble
LD011	Dolomitic marble	131	Light grey, massive, microsparite dolomitic marble (Fig. 5I)
LD012	Dolomitic marble	104	Grey, massive, locally recrystallized, microsparite dolomitic marble
LD013	Dolomitic marble	41	Grey, massive, microsparite dolomitic marble, with a few carbonate veinlets
LD014	Dolomitic marble	0	Light grey, notably silicified, massive, microsparite dolomitic marble, with some carbonate veinlets
Pailou			
HLD01	Magnesite		White, medium-grained, massive magnesite, with scattered algal spots
HLD02	Magnesite		Pink, coarse sub-equigranular grained, massive magnesite (Fig. 5E)
HLD03	Magnesite		Light grey, coarse-grained, banded magnesite (Fig. 5C)
HLD04	Magnesite		Pink, coarse sub-equigranular grained, massive magnesite
HLD05	Magnesite		Pink, coarse sub-equigranular grained, massive magnesite
HLD06	Magnesite		Pink, coarse sub-equigranular grained, massive magnesite
HLD07	Magnesite		Light grey, medium-grained, massive magnesite
HLD08	Magnesite		White, fine-grained, massive magnesite

4. RESULTS

The analytical data on major elements and carbon and oxygen isotope ratios are presented in Tables 2 and 3, respectively. The strata examined in this study (Qingshanhuai area) cover a total thickness of 1144 m and consist of two major petrologic domains. The upper part is *ca.* 550 m thick and dominated by magnesite; while the lower part is 600 m thick and comprises dolomitic marbles. Microlithological features of representative samples from the Dashiqiao magnesite belt are shown in Figure 5 and the stratochemical variations are presented in Table 2 and discussed by Tang *et al.* (2009). The $\delta^{13}C$ histogram (Fig. 6a) shows a unimodal distribution whereas the $\delta^{18}O$ values (Fig. 6b) show scatter.

The $\delta^{13}C$ and $\delta^{18}O$ values of the dolomitic marbles show a range of 0.6−1.4‰ and 16.4−19.5‰, respectively. The CaO and MgO concentrations are 27.77−28.49% and 21.47−22.88%, respectively, with CaO/MgO ratios (mol) of 0.87−0.94 and LOI (weight loss between 120−900 °C) of 45.95−47.06%. The MnO, $Fe_2O_3^T$, Al_2O_3, Na_2O and P_2O_5 concentrations are lower than 1%, with values of 0.01−0.02%, 0−0.08%, 0.38−0.76%, 0.29−0.33% and 0.017−0.058%, respectively. The SiO_2 content ranges from 1.61% to 2.88%.

The magnesite rocks have CaO and MgO contents of 0.33−11.83% and 36.43−46.65%, respectively. Their LOI values range 47.20−59.12%, clearly higher than those of dolomitic marbles, indicating the increase of $MgCO_3$ in the rocks. Compared to dolomitic marbles, they have lower $\delta^{13}C$ (−1.3−0.9‰) and $\delta^{18}O$ (9.2−16.9‰; Table 3), as well as depleted Na_2O (0.01−0.28%), but higher MnO (0.025−0.087%) and $Fe_2O_3^T$ (0.30−1.02%). The SiO_2 (0.12−3.98%) and P_2O_5 (0.011−0.047%) as well as Al_2O_3 (0.12−3.98%) values are lower and more variable than those of the dolomites. Concentrations of K_2O and TiO_2 in the magnesite samples are even lower than the detection limit.

5. DISCUSSION

5.1. Post-depositional variation in $\delta^{13}C$ and $\delta^{18}O$

Carbon and oxygen isotopes of carbonate rocks can be reset during post-depositional diagenetic, metamorphic and

Table 2. Chemical compositions (wt%) of the Dashiqiao Formation, Dashiqiao magnesite belt

Sample no.	SiO_2	Al_2O_3	$Fe_2O_3{}^T$	CaO	MgO	K_2O	Na_2O	MnO	TiO_2	P_2O_5	LOI	Total	Mg/Ca
Qingshanhuai													
LD001	3.20	1.43	1.02	26.98	21.95	<0.01	0.31	0.07	0.03	0.04	44.92	99.97	1.14
LD006	1.13	0.38	1.01	4.53	42.42	<0.01	0.26	0.10	<0.001	0.03	50.12	99.98	13.16
LD002	3.98	0.32	1.02	0.45	46.65	<0.01	0.25	0.09	<0.001	0.02	47.20	99.98	142.86
LD003	2.06	0.37	0.61	0.33	46.63	<0.01	0.24	0.08	<0.001	0.05	49.61	99.98	200.00
LD004	1.23	0.39	0.76	11.72	36.68	<0.01	0.28	0.05	<0.001	0.04	48.83	99.98	4.35
LD005	1.37	0.38	0.55	11.83	36.43	<0.01	0.28	0.04	<0.001	0.03	49.07	99.98	4.35
LD007	1.01	0.38	0.72	7.61	40.14	<0.01	0.27	0.04	<0.001	0.02	49.80	99.98	7.14
LD008	1.21	0.33	0.91	7.37	40.17	<0.01	0.26	0.05	<0.001	0.01	49.67	99.98	7.69
Average ($n=6$)	1.81	0.36	0.76	6.55	41.12		0.26	0.06		0.03	49.03	99.98	8.33
$\pm1\sigma$	1.12	0.03	0.18	5.14	4.57		0.02	0.02		0.01	0.97	0.00	87.39
LD009	1.74	0.47	0.00	27.77	22.88	<0.01	0.29	0.01	<0.001	0.06	46.76	99.98	1.15
LD010	2.60	0.76	0.12	28.31	21.47	<0.01	0.33	0.02	0.00	0.03	46.36	99.99	1.06
LD011	2.00	0.51	0.03	28.49	21.74	<0.01	0.31	0.01	<0.001	0.03	46.86	99.98	1.06
LD012	1.61	0.39	0.03	27.93	22.62	<0.01	0.30	0.02	<0.001	0.02	47.06	99.98	1.14
LD013	1.97	0.39	0.03	28.14	22.37	<0.01	0.31	0.01	<0.001	0.05	46.71	99.99	1.11
LD014	2.88	0.38	0.08	28.21	22.12	<0.01	0.31	0.01	<0.001	0.02	45.95	99.96	1.10
Average ($n=6$)	2.13	0.48	0.05	28.14	22.20		0.31	0.01		0.03	46.62	99.98	1.10
$\pm1\sigma$	0.50	0.15	0.04	0.26	0.53		0.01	0.00		0.02	0.40	0.01	0.04
Pailou													
HLD01	3.88	0.36	0.49	0.63	43.26	0.01	0.03	0.04	0.00	0.04	51.16	99.91	86.77
HLD02	0.22	0.09	0.71	1.54	45.20	0.01	0.01	0.06	0.00	0.49	51.56	99.89	140.87
HLD03	1.34	0.66	0.72	0.40	44.05	0.01	0.02	0.08	0.07	0.09	51.92	99.35	37.30
HLD04	1.38	0.07	0.45	0.71	38.05	0.02	0.01	0.03	<0.001	0.11	59.12	99.94	67.91
HLD05	2.30	1.00	0.54	1.22	40.25	0.03	0.01	0.03	0.03	0.53	50.94	96.89	41.93
HLD06	3.54	0.05	0.30	0.42	43.99	0.01	0.02	0.04	<0.001	0.04	51.49	99.90	132.34
HLD07	0.17	0.07	0.47	0.73	46.35	0.02	0.01	0.03	0.00	0.09	51.97	99.91	81.14
HLD08	0.12	0.07	0.39	0.52	42.65	0.01	0.01	0.03	<0.001	0.02	56.13	99.95	104.48
Average ($n=8$)	1.62	0.30	0.51	0.77	42.98	0.01	0.02	0.04	0.01	0.18	53.04	99.47	86.59
$\pm1\sigma$	1.50	0.36	0.15	0.40	2.68	0.01	0.01	0.02	0.03	0.21	2.96	1.06	38.10

hydrothermal alteration processes, which usually lead to isotopic fractionation and a decrease in the $\delta^{13}C$ and $\delta^{18}O$ values (Veizer and Hoefs, 1976; Valley, 1986; Guerrera *et al*., 1997; Jacobsen and Kaufman, 1999; Ray *et al*., 2003; Banner, 2004; Melezhik *et al*., 2005a; Qi *et al*., 2005). To investigate the primary isotopic signature of the carbonates, any impact from post-depositional diagenetic processes must consequently be considered and identified.

Veizer *et al*. (1999) suggested that diagenetic resetting was mostly related to the generation of stable mineralogical assemblages during the early burial history of the sediments. This process results in an average of ~2‰ $\delta^{18}O$ depletion, but once accomplished, the bulk system represented by the matrix remains internally buffered and is thus relatively inert to further resetting. Oxygen isotope ratios of 260 Precambrian limestones and dolomites documented by Schidlowski *et al*. (1975) showed that high-grade metamorphosed or severely recrystallized marbles were depleted in $\delta^{18}O$ by 2–3‰ on average, compared to essentially unaltered contemporaneous carbonates.

Valley (1986), Schidlowski (1988), Chen *et al*. (2000), and Bekker and Kaufman (2007) showed that metamorphism could cause isotopic exchange between carbonates and organisms leading to $\delta^{13}C$ depletions of the former and $\delta^{13}C$ enrichments of the latter. The studies by Baker and Fallick (1989a, b) and Melezhik *et al*. (2001a, b) suggest that the oxygen and carbon isotopic values are negatively correlated with the degree of metamorphism. Whereas the ^{13}C-enrichment signature could be retained in amphibolite facies carbonates, the imprint nearly disappears in granulite facies rocks. For instance, the $\delta^{13}C$ value of the ~2.0 Ga Lofoten–Vesteraten marbles is depleted by >8‰ on average while passing from amphibolite facies (7.5 ± 2.9) to granulite facies (-1.5 ± 4.3), with a decrease in $\delta^{18}O$ from ~25‰ to ~10‰ (Baker and Fallick, 1989b; Fig. 7; Table 4). Bottinga (1969), Wada and Suzuki (1983), and Schidlowski (1988) noted that metamorphism at temperatures >650 °C would result in a decrease in ^{13}C by more than 3‰. Banner and Hanson (1990) showed that the $\delta^{18}O$ values of dolomites of the Mississippian Burlington–Keokuk Formation varied extensively with the water–rock interaction, whereas $\delta^{13}C$ and rare earth elements were unaffected. The oxygen isotope system of carbonates is more sensitive to post-depositional resetting than the carbon

Table 3. Carbon and oxygen isotope ratios (‰) of samples from the Dashiqiao Formation, Liaohe Group

No.	Sample geology	$\delta^{13}C_{V\text{-}PDB}$	$\delta^{18}O_{V\text{-}PDB}$	$\delta^{18}O_{V\text{-}SMOW}$	Data source
LD001	Talc-dolomitic marble	−2.6	−16.2	14.1	This study
LD002	Magnesite	0.1	−17.5	12.7	This study
LD003	Magnesite	0.6	−17.8	12.5	This study
LD004	Magnesite	0.5	−19.8	10.3	This study
LD005	Magnesite	0.3	−20.8	9.2	This study
LD006	Veinlet-filled magnesite	−2.7	−14.1	16.2	This study
LD007	Magnesite	0.4	−20.0	10.1	This study
LD008	Magnesite	0.2	−19.7	10.4	This study
LD009	Dolomitic marble	1.2	−12.9	17.4	This study
LD010	Dolomitic marble	1.4	−11.7	18.7	This study
LD011	Dolomitic marble	1.4	−11.0	19.5	This study
LD012	Dolomitic marble	1.4	−11.3	19.1	This study
LD013	Dolomitic marble	0.6	−12.4	18.0	This study
LD014	Dolomitic marble	1.2	−14.0	16.4	This study
HLD01	Magnesite	−1.1	−15.8	14.7	This study
HLD02	Magnesite	0.5	−15.6	14.9	This study
HLD03	Banded magnesite	−1.3	−14.4	16.1	This study
HLD04	Magnesite	0.2	−15.4	15.0	This study
HLD05	Magnesite	0.9	−15.4	15.1	This study
HLD06	Magnesite	0.1	−13.6	16.9	This study
HLD07	Magnesite	0.6	−16.3	14.1	This study
HLD08	Magnesite	0.4	−16.3	14.1	This study
DSQ2	Marble	−0.6		17.3	Jiang *et al*. (2004)
DSQ6-1	Marble	1.0		18.5	Jiang *et al*. (2004)
DSQ11	Marble	0.1		12.6	Jiang *et al*. (2004)
DSQ19-2a	Marble	−1.9		16.3	Jiang *et al*. (2004)
M-1	Marble	−0.6		15.5	Jiang (1987)
L01015	Calcite marble	−1.8		22.8	Chen *et al*. (2003a)
L01025	Calcite marble	−4.5		19.6	Chen *et al*. (2003a)
L01017	Stromatolite marble	−0.5		20.2	Chen *et al*. (2003a)
L01020	Banded marble	4.4		18.2	Chen *et al*. (2003a)
L01021	Banded marble	0.8		11.2	Chen *et al*. (2003a)
L01022	Magnesite	1.2		12.6	Chen *et al*. (2003a)
L01023	Banded magnesite	−0.8		12.1	Chen *et al*. (2003a)
L01035	Talc magnesite	−1.4		11.1	Chen *et al*. (2003a)
DSQ14	Magnesite	0.4		11.1	Jiang *et al*. (2004)
DSQ15	Magnesite	−0.4		13.8	Jiang *et al*. (2004)
HYZ6-1	Magnesite	1.2		9.6	Jiang *et al*. (2004)
M-2	Magnesite	−1.3		11.7	Jiang (1987)
M-3	Magnesite	−0.6		11.1	Jiang (1987)
DSQ19-1	Magnesite vein	0.3		5.2	Jiang *et al*. (2004)
DSQ19-2b	Magnesite vein	0.2		8.0	Jiang *et al*. (2004)
M-4	Calcite vein	1.3		16.9	Jiang (1987)

isotope system and can serve as an indicator of hydrothermal alterations (Tang *et al*., 2011).

Some studies have attempted to use $\delta^{18}O$ values to identify whether carbonates have undergone hydrothermal alteration. Veizer *et al*. (1992) noted that a low $\delta^{18}O$ value indicated equilibrium reactions between primary rocks and fluids. Feng *et al*. (2003) and Aharon (2005) showed that the minimum $\delta^{18}O$ value of carbonates is not lower than 18‰ if post-depositional modification processes do not reset the isotope system. Melezhik *et al*. (2005b) suggested that this minimum $\delta^{18}O$ value should be at least 20‰. Other researchers have conducted studies to determine why the $\delta^{18}O$ of carbonates is more variable than $\delta^{13}C$ (Banner and Hanson, 1990; Jacobsen and Kaufman, 1999; Ray *et al*., 2003). Banner and Hanson (1990) and Jacobsen and Kaufman (1999) noted that during open system diagenesis, calcite equilibrates with fluid $\delta^{18}O$ values at fluid/rock ratios (mol) three orders of magnitude lower (<10) than the fluid/rock ratios at which it equilibrates with fluid $\delta^{13}C$ values (10^3), due to the extreme differences in the concentrations of O and C in carbonates and fluids. Furthermore, the carbon isotopes may be strongly buffered by the high C concentrations in carbonate minerals relative to the fluid (Banner and Hanson, 1990; Jacobsen and Kaufman, 1999, Melezhik *et al*.,

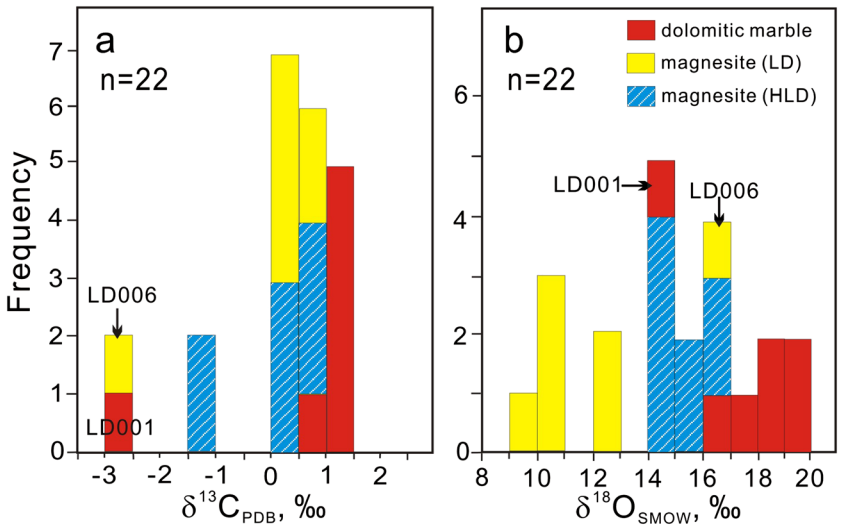

Figure 6. Histograms for $\delta^{13}C$ (**a**) and $\delta^{18}O$ (**b**) values of the Dashiqiao Formation, Qingshanhuai and Pailou areas.

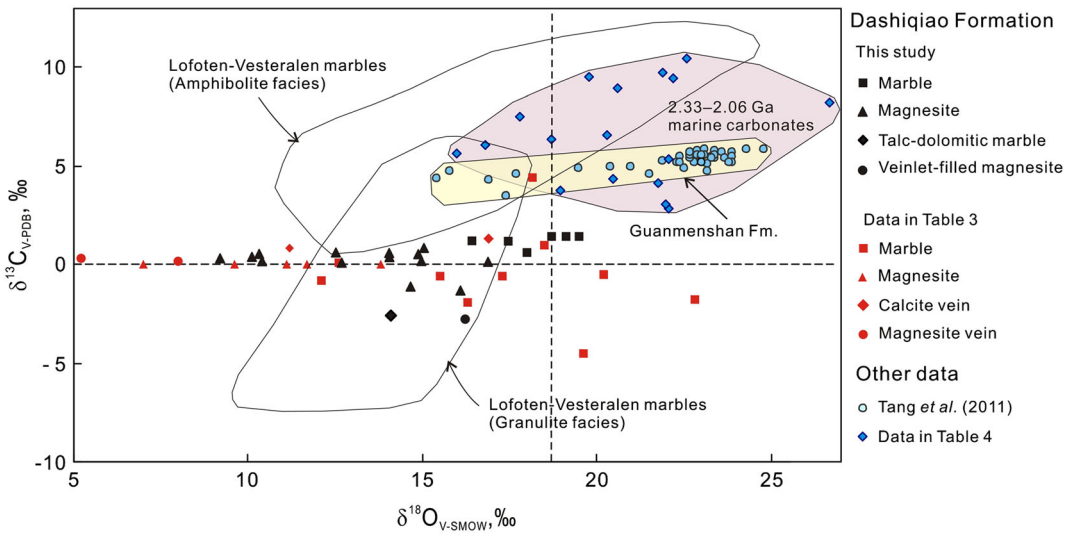

Figure 7. $\delta^{13}C$ and $\delta^{18}O$ values of the Dashiqiao Formation and 2.33−2.06 Ga marine carbonates. Data source: Lofoten–Vesteraten marbles (Baker and Fallick, 1989b); dolomites of the Guanmenshan Formation (Tang *et al.*, 2011); 2.33−2.06 Ga marine carbonates (see Table 4).

2006) and, consequently, infiltration of externally sourced fluids is likely to have a relatively greater effect on the O isotope compositions in carbonate rocks (Ray *et al.*, 2003; Melezhik *et al.*, 2006, 2008; Tang *et al.*, 2011).

The carbon and oxygen isotopes of carbonate sediments generally tend to decrease during post-depositional diagenetic, metamorphic and hydrothermal alteration processes as evident from the above studies, leading to three major geochemical trends in $\delta^{13}C$ versus $\delta^{18}O$ plots. (i) Both $\delta^{13}C$ and $\delta^{18}O$ decrease non-linearly to produce a scatter pattern (Bekker *et al.*, 2005; Melezhik *et al.*, 2005b) that is a common characteristic for most carbonates (Veizer and Hoefs, 1976) and indicates isotopic equilibration with fluids due to hydrothermal alteration or diagenetic–metamorphic modification at a high fluid/rock ratio (Guerrera *et al.*, 1997; Jacobsen and Kaufman, 1999). (ii) A trend nearly parallel to the oxygen axis that demonstrates partial isotope resetting caused by lower fluid/rock ratio fluid alteration (Banner and Hanson, 1990). (iii) A rare trend essentially parallel to the $\delta^{13}C$ axis that is interpreted by Melezhik *et al.* (2005b) to reflect intense alteration in an open system with a high fluid/rock ratio. The latter trend is further believed to be a unique phenomenon recording alteration of carbonate strata by carbonic fluid flow (Tang *et al.*, 2011). In addition, diagenetic processes would lead to decrease in Sr concentration and increases in Mn, Fe and

Table 4. The $\delta^{13}C$ and $\delta^{18}O$ averages of carbonate strata with age of 2.33−2.06 Ga (bracketed are variations)

Location	Name of carbonate strata	$\delta^{13}C_{carb}$	$\delta^{18}O_{carb}$	*n*	Age (Ga)	Data sources
Global	Archaean to Palaeoproterozoic dolostones		26 ± 2‰		Ar-PaleoPt	Veizer *et al*. (1992)
N. Amer.	Slaughterhouse Fm., Sierra Madre, Wyoming	9.5 ± 4.1 (5.9–16.6)	19.8 ± 3.1 (15.8–26.5)	8	PaleoPt	Bekker *et al*. (2003a)
N. Amer.	Nash Fork Fm., Medicine Bow Mts, Wyoming	(3.1–28.2)	(12.9–27.3)	104	PaleoPt	Bekker *et al*. (2003a)
N. Amer.	Whalen Gp. carbonates, Hartville Uplift, Wyoming	3.0 ± 2.8 (−0.3–8.2)	22.0 ± 2.8 (15.4–26.5)	36	PaleoPt	Bekker *et al*. (2003a)
N. Amer.	Kona dolomite, Chocolay Gp., Marquette Range SGp., Marquette Trough, Upper Peninsula Michigan, USA	6.3 ± 1.4 (1.9–9.5)	18.7 ± 2.1 (13.2–24.3)	107	2.29–2.20	Bekker *et al*. (2006)
N. Amer.	Gorden Lake Fm., Cobalt Gp., Huronian SGp., Ontario, Canada	5.4 ± 1.7 (1.3–8.2)	18.1 ± 2.2 (12.7–22.0)	40	2.45–2.22	Bekker *et al*. (2006)
N. Amer.	Dunphy, Portage Fm., Pistolet subgroup, and Alder, Uvé Fm., Konblake Gp., Kaniapiskau SGp., Labrador Trough, Canada	9.7 ± 2.8 (5.3–15.4)	21.9 ± 2.6 (16.2–25.4)	23	2.17–2.14	Melezhik *et al*. (1997)
S. Amer.	Cercadinho Fm., Piracicaba Gp., Minas SGp., Iron Quadrangle, Brazil	4.1 ± 0.5 (3.3–5.4)	21.8 ± 0.7 (20.7–22.6)	11	2.42–2.11	Bekker *et al*. (2003b)
		3.9 ± 0.3 (3.3–4.2)	21.9 ± 0.7 (20.7–22.6)	9	2.42–2.11	Maheshwari *et al*. (2010)
S. Amer.	Fecho doFunil Fm., Piracicaba Gp., Minas SGp., Iron Quadrangle, Brazil	6.5 ± 0.3 (5.6–7.4)	20.3 ± 0.7 (18.2–21.5)	69	2.11 ± 0.11	Bekker *et al*. (2003b)
		6.3 ± 0.2 (5.8–6.9)	20.6 ± 0.4 (19.5–21.2)	48	2.11 ± 0.11	Maheshwari *et al*. (2010)
S. Amer.	PasoSeverino Fm., Piedra Alta Terrane, Río de la Plata craton, Uruguay	3.6 ± 4.0 (−5.6–11.6)	18.3 ± 5.3 (8.4–26.8)	31	~2.15	Maheshwari *et al*. (2010)
Europe	Lewisian limestone, Lewisian province, Scotland	5.6 ± 5.6 (−3.9–12.9)	16.0 ± 3.2 (9.4–22.0)	19	~2.1	Baker and Fallick (1989a)
Europe	Lofoten–Vesteralen Marble, Norway (granulite facies)	−1.5 ± 4.3 (−7–6.4)	14.1 ± 1.8 (9.9–17.9)	28	~2.0	Baker and Fallick (1989b)
Europe	Lofoten–Vesteralen Marble, Norway (amphib. facies)	7.5 ± 2.9 (0.6–12.1)	17.8 ± 3.3 (11.2–24.2)	40	~2.0	Baker and Fallick (1989b)
Europe	Kuusamo Fm. sericite schist, Finland	8.1 ± 0.1	~23.8	2	2.25 ± 0.05	Karhu (1993)
Europe	Sompujarvi Fm., Finland	7.3 ± 1.2		3	2.25 ± 0.04	Karhu (1993)
Europe	Misi dolomite stratum, Finland	12.6 ± 0.4		5	2.23 ± 0.07	Karhu (1993)
Europe	Lower Viistola Fm., Finland	10.0 ± 0.7		5	2.113 ± 0.004	Karhu (1993)
Europe	Jouttiaapa Fm., Finland	8.4 ± 1.6		10	2.09 ± 0.07	Karhu (1993)
Europe	Upper Petonen Fm., Finland	2.0 ± 1.4		2	2.062 ± 0.002	Karhu (1993)
Europe	Karelian dolomite, Fennoscandian	4.3 ± 1.1 (3.1–8.6)	20.5 ± 2.7 (17.7–23.6)	8	2.2–1.9	Schidlowski *et al*. (1975)
Europe	Yatulian Series, Kirelia	(3.5–13.7)		22	~2.3	Tikhomirova and Makarakhin (1993)
Africa	Francevillian Series, Francevillian province, Gabon	4.3 ± 1.6		4	2.07 ± 0.05	Gauthier-Lafaye and Weber (1989)
Africa	Lomagundi Gp., Rhodesia	9.4 ± 2.0 (2.2–13.4)	22.2 ± 1.6 (18.5–24.6)	11	2.65–1.95	Schidlowski *et al*. (1975)
Africa	Lomagundi Gp., Rhodesia	8.2 ± 2.6 (2.6–13.6)	~26.9	67	2.07 ± 0.10	Schidlowski *et al*. (1976)
S Africa	Duitschland Fm., Chuniespoort Gp., Transvaal SGp	6.4 ± 2.8 (3.6–9.3)	(14.3–20.6)	33	2.43–1.93	Buick *et al*. (1998)
S Africa	Silverton Shale Fm., Pretoria Gp., Transvaal SGp.	8.5 ± 3.1 (3.8–10.7)	(15.6–23.2)	39	2.22–1.93	Buick *et al*. (1998)
S Africa	Upper Duitschland Fm., Lower Pretoria Gp., Transvaal SGp.	6.0 ± 3.0 (−2.0–10.1)	16.8 ± 3.6 (11.6–23.9)	24	2.480–2.322	Bekker *et al*. (2001)
S Africa	Tongwane Fm., Lower Pretoria Gp., Transvaal SGp.	2.8 ± 0.6 (1.9–3.5)	22.1 ± 1.0 (21.1–23.5)	5	2.480–2.322	Bekker *et al*. (2001)
S Africa	Lucknow Fm., Olifantshoek Gp., Grigualand West Basin	(10.3–10.5)	(22.3–22.8)	2	2.222–1.928	Bekker *et al*. (2001)
Africa	Pretoria Gp.	0.8 ± 0.6		3	2.22 ± 0.02	Walravan *et al*. (1990)
S Asia	Jhamarkotra Fm., Aravalli SGp., NW India	8.9 ± 1.7 (5.1–11.1)	20.6 ± 1.3 (18.6–23.2)	15	2.20–1.90	Sreenivas *et al*. (2001)
		(−3–11.9)		78	~2.15	Purohit *et al*. (2010)
Australia	Juderina Fm., Yerrida basin, Western Australia	(9.0–9.4)		?	2.173 ± 0.064	EI Tabakh *et al*. (1999)
E Asia	Guangmenshan Fm., Liaohe Gp, Liangning, China	5.3 ± 0.5 (3.5–5.9)	22.1 ± 2.3 (15.8–24.8)	42	2.3–1.85	Tang *et al*. (2011)
E Asia	Dashiqiao Fm. dolomite, Liaohe Gp, Liangning, China	1.2 ± 0.3 (0.6–1.4)	18.2 ± 1.1 (16.4–19.5)	6	2.2–2.174	This paper
E Asia	Dashiqiao Fm. magnesite, Liaohe Gp, Liangning, China	0.4 ± 0.2 (0.1–0.9)	12.9 ± 2.5 (9.2–16.9)	12	2.2–2.174	This paper

Rb concentrations of carbonates (Derry *et al.*, 1992; Veizer *et al.*, 1992, 1999; Melezhik *et al.*, 2008; and references therein), which can also serve as an important criterion for identifying post-depositional alterations.

5.2. *Isotope signature in Dashiqiao Formation and its implications*

In Figure 8, the $\delta^{13}C$ and $\delta^{18}O$ values of the carbonates from the Dashiqiao Formation show a fairly positive correlation (excluding samples LD001 and LD006, discussed below) with a trend nearly parallel to the oxygen axis in $\delta^{13}C-\delta^{18}O$ plots, indicating diagenetic, metamorphic and/or fluid alteration at lower fluid/rock ratios in the initial stage. The wide $\delta^{13}C$ and $\delta^{18}O$ variations indicate that the post-depositional geological processes were complex and heterogeneous. The dolomitic marbles and magnesites have differing $\delta^{13}C$ and $\delta^{18}O$ values, reflecting a genetic difference between the two.

The average $\delta^{18}O$ value of the 2.33–2.06 Ga global carbonate strata is ~22‰ (Table 4, Fig. 7). Veizer *et al.* (1992) noted that the mean $\delta^{18}O$ value of early Precambrian (>1.9 Ga) dolomites is 26 ± 2‰. Thus, the $\delta^{18}O$ values of primary Palaeoproterozoic dolomite are generally >22‰, such as the 2.3–1.9 Ga dolomites within the Guanmenshan Formation, Liaohe Group, northern Liaoning (Tang *et al.*, 2011) with a $\delta^{18}O$ average of 22.1 ± 2.3‰. The $\delta^{18}O$ values of the 2.2–2.174 Ga Dashiqiao carbonates range from 9.2–19.5‰ with average of 14.8 ± 3.0‰ ($n = 22$), notably lower than those of global contemporaneous dolomite (Fig. 7), with the degree of depletion being similar to those of the Lofoten–Vesteraten marbles from amphibolite to granulite facies (Baker and Fallick, 1989b). Chen *et al.* (2003a, b) and Jiang *et al.* (2004) argued that the isotope signatures of the Dashiqiao Formation witnessed extensive diagenetic and metamorphic overprints. Since the grade of metamorphism of the Liaohe Group is only up to greenschist or amphibolite facies, the extent of $\delta^{18}O$ depletion in the Dashiqiao Formation cannot be interpreted by solely considering diagenetic–metamorphic alteration, and the impact of hydrothermal alteration must also be taken into account. As shown in Figure 8b–f, from dolomitic marble through massive magnesite to veinlet-filled magnesite, the MgO/CaO ratios of the samples increase by two orders of magnitude, the Mn concentrations increase by one order of magnitude, and Fe concentrations increase by about two orders of magnitude. Moreover, both Mn and Fe are negatively correlated with $\delta^{13}C$ (Fig. 8b, c), which indicate that the Dashiqiao Formation was subjected to significant fluid alteration, especially, by meteoric water.

In Table 3, apart from LD001 and LD006 (see Section 5.3), the $\delta^{18}O$ values of 14 magnesite samples range from 9.2–16.9‰ (average 13.3 ± 2.5), notably lower than those of six dolomitic marbles (16.4–19.5‰, average 18.2 ± 1.1), which suggests that the magnesites have experienced stronger hydrothermal alteration than the dolomitic marbles. Even if we

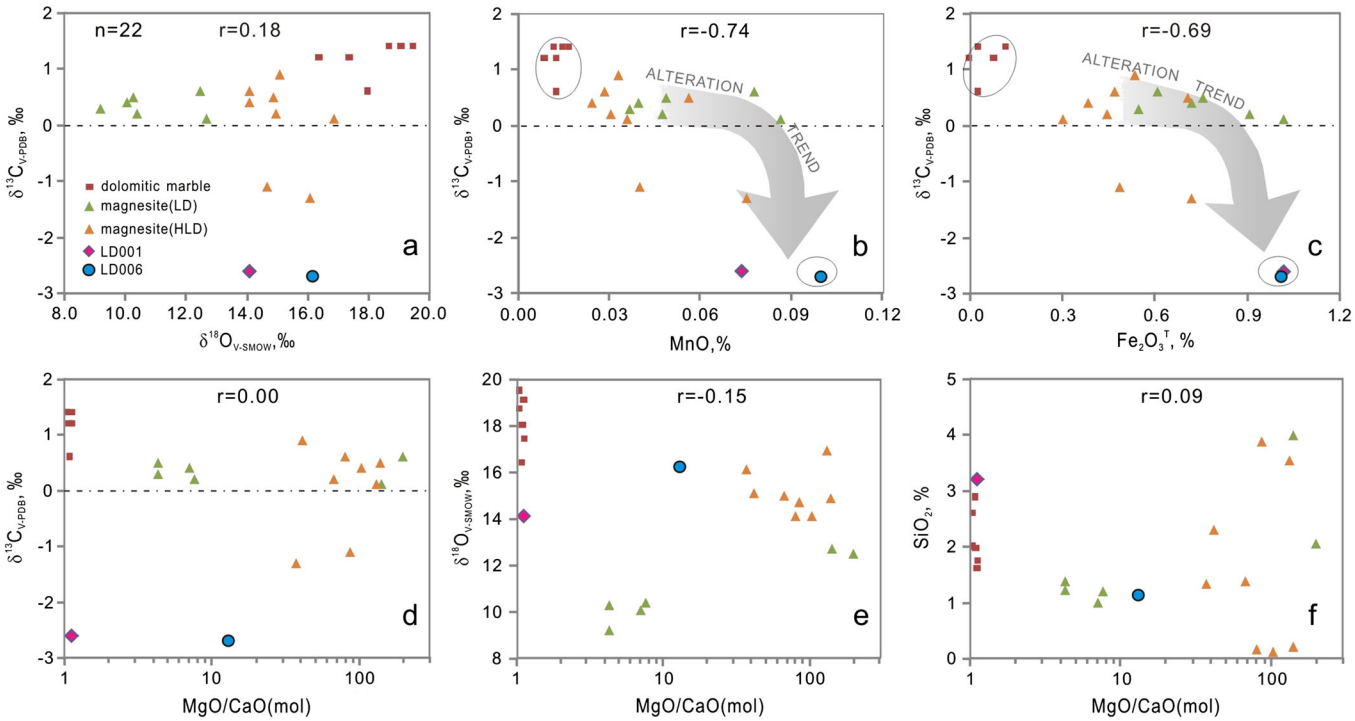

Figure 8. Correlations of $\delta^{13}C$ with $\delta^{18}O$ (**a**), MnO (**b**), $Fe_2O_3^T$ (**c**) and MgO/CaO (**d**), as well as correlations of MgO/CaO with $\delta^{18}O$ (**e**) and SiO_2 (**f**) of the Dashiqiao Formation, Qingshanhuai and Pailou areas. This figure is available in colour online at wileyonlinelibrary.com/journal/gj

consider only the impact of diagenesis which usually causes ~2‰ depletion in $\delta^{18}O$ (Veizer *et al*., 1999), the initial $\delta^{18}O$ value of the Dashiqiao carbonates is estimated >21.5‰ (19.5 + 2). This estimation is still lower than the highest $\delta^{18}O$ value (22.8‰) of the Dashiqiao Formation marbles reported by Chen *et al*. (2003a, b). We therefore infer that the initial $\delta^{18}O$ of the Dashiqiao Formation carbonates might have been similar to those of the Guanmaenshan Formation carbonates (25 ± 1‰; Tang *et al*., 2011).

Since the decrease in $\delta^{18}O$ is accompanied by a concomitant decrease in $\delta^{13}C$ (Fig. 8a), the initial $\delta^{13}C$ values of the Dashiqiao Formation carbonates must have been higher than the measured values. In Figures 6 and 8, the $\delta^{13}C$ values of the 12 magnesite samples are positive, with an average of 0.4 ± 0.2‰, and show a slightly positive anomaly. The $\delta^{13}C$ values of six massive dolomitic marbles of wall rocks are 0.6−1.4‰ (average 1.2 ± 0.3‰), higher than the average of marine carbonates (0.5‰; Schidlowski, 2001; Hoefs, 1997), indicating that the Dashiqiao Formation must have possessed remarkably positive $\delta^{13}C$ anomalies before diagenesis, metamorphism and hydrothermal alteration. We consider the different possibilities to account for the above features. (i) Granulite facies metamorphism could result in a depletion in $\delta^{13}C$ of >8‰ on average compared to those of amphibolite facies carbonates (Baker and Fallick, 1989b), and the degree of $\delta^{18}O$ depletion of the studied carbonates is equivalent to the depletion caused by granulite facies metamorphism. (ii) Metamorphism at temperatures >650°C could result in >3‰ decrease in $\delta^{13}C$ (Bottinga, 1969; Wada and Suzuki, 1983; Schidlowski, 1988), and the Liaohe Group generally underwent greenschist to amphibolite facies metamorphism, as well as extensive hydrothermal alteration, which must have caused a great decrease in $\delta^{18}O$. (iii) The wide variations in $\delta^{18}O$ and $\delta^{13}C$ values of the Dashiqiao Formation carbonates suggest that fluid–rock interaction resulted in significant depletion in $\delta^{18}O$ and $\delta^{13}C$. We extrapolate this to infer that the initial $\delta^{13}C$ values of the Dashiqiao Formation carbonates were no less than +4.2‰, and decreased by at least 3‰ during post-depositional processes. This inference is also supported by the highest $\delta^{13}C$ value of 4.4‰ obtained from the Dashiqiao dolomitic marbles by Chen *et al*. (2003a, b) (Fig. 7). Thus, it is concluded that the $\delta^{13}C$ values of the Dashiqiao Formation carbonates show a remarkable positive excursion, indicating that the Jiao-Liao-Ji Belt of the North China Craton preserves the GOE at 2.33−2.06 Ga.

5.3. *Formation of the Dashiqiao magnesite deposits*

The genesis of the Dashiqiao giant magnesite belt has been addressed in various works (Zhang *et al*., 1988; Dong *et al*., 1996; Chen and Cai, 2000; Chen *et al*., 2003a, b; Jiang *et al*., 2004). Our study shows that the magnesite deposits in the Dashiqiao magnesite belt were formed through a complex processes as follows: (i) Palaeoproterozoic sedimentation in a high-Mg lagoonal environment (Jiang *et al*., 2004), with evaporation leading to an enrichment of Mg, ^{18}O and ^{13}C in the primary carbonates. Tu (1996) noted that Palaeoproterozoic Mg-rich seawater and CO_2-rich atmosphere contributed to the formation of the magnesite deposits; (ii) post-depositional diagenesis, probably accompanied with Mg-rich brine metasomatism similar to modern sabkha evaporation (Jiang *et al*., 2004); (iii) greenschist to amphibolite facies metamorphism of the Liaohe Group and related metamorphic fluid alteration resulting in chemical differentiation, possible Mg-enrichment and recrystallization of magnesite ores (Zhang *et al*., 1988; Dong *et al*., 1996; Chen and Cai, 2000); these also led to a reduction in the $\delta^{18}O$ and $\delta^{13}C$ ratios of the magnesite ores, which are lower than those of both the footwall dolomites at Qingshanhuai (Table 3; Figs. 7 and 8) and the contemporaneous global carbonate strata (Table 4, Fig. 7) and (iv) Local post-metamorphic hydrothermal alterations, as reflected by the formation of fine vein-type samples LD001 and LD006, probably associated with faulting, causing further decrease in $\delta^{18}O$ and $\delta^{13}C$ ratios. Among the four processes mentioned above, the first three were addressed in previous studies, but the last one has not been discussed yet.

The sample LD001 has a similar Mg/Ca ratio to those of footwall dolomitic marbles, but has the lowest $\delta^{13}C$ (−2.6‰) and $\delta^{18}O$ (14.1‰) values among all the dolomitic marbles studied, with low Mg/Ca ratios (1.06−1.15) (Fig. 8d, e). This sample was collected from a fault zone between the hanging-wall dolomitic marble and magnesite orebody and is characterized by the presence of mega-crystals of cylindrical talc (Table 1; Fig. 5D). The talc was possibly formed by interaction between dolomite and siliceous hydrothermal fluids, or between argillaceous dolomite and hydrothermal fluids through the reaction:

$$3CaMg(CO_3)_2 + 4SiO_2 + H_2O \rightarrow Mg_3[Si_4O_{10}](OH)_2(\text{talc}) + 3CaCO_3 + 3CO_2\uparrow$$

The release of CO_2 resulted in a decrease in both $\delta^{13}C$ and $\delta^{18}O$ of dolomite, since the CO_2 liberated during the reaction is about 5‰ richer in ^{18}O and about 6‰ richer in ^{13}C than the coexisting calcite (Shieh and Taylor, 1969). Hence, the lower $\delta^{13}C$ and $\delta^{18}O$ values of sample LG001 and the formation of cylindrical talc mega-crystals can be interpreted to have resulted from local hydrothermal alteration. A talc-bearing magnesite obtained from the Dashiqiao Fm. by Chen *et al*. (2003a) has also shown lower $\delta^{13}C$ (−1.4‰) and $\delta^{18}O$ (11.1‰) values (Table 3).

Sample LD006 (Fig. 5G, H) is from pink, coarse-grained magnesite ore, which is developed with micrograined, fine carbonate veinlets. It has the highest Fe and Mn concentrations (Fig. 8b, c) among all the magnesite samples, indicating that it experienced local fluid–rock interaction after the

formation of the massive magnesite. Minerals in sample LD006 are dominated by magnesite, with minor chalcedony and disseminated limonite, suggesting that the post-ore fluid–rock interaction was possibly resulted from low-temperature meteoric water circulation. Sample LD006 has the lowest $\delta^{13}C$ value (−2.7‰) among all the samples, which can be reasonably interpreted by referring to the mechanism for sample LD001. However, LD006 has a higher $\delta^{18}O$ value (16.2‰) than the other magnesite ores and sample LD001 (Table 3; Fig. 8a, e), which warrants further discussion.

During the interaction between fluid and rock, the isotopic fractionation is mainly controlled by temperature. The final $\delta^{13}C$ and $\delta^{18}O$ values in rocks are controlled by the initial isotope compositions of rocks and fluid. Given that sample LD006 ($\delta^{18}O = 16.2‰$; $\delta^{13}C = -2.7‰$) was isotopically equilibrated with fluids at a given temperature, we can estimate the possible temperature and isotope compositions of fluids through calculation using equations of (1) $10^3 1n\alpha_{(Dolomite-water)} = 3.06 \times 10^6/T^2 - 3.24$ (Matthews and Katz, 1977) and (2) $10^3 1n\alpha_{(Dolomite-CO2)} = -0.388\ 10^9/T^3 + 5.538 \times 10^6/T^2 - 11.346 \times 10^3/T + 3.132$ (Sheppard and Schwarcz, 1970). Table 5 lists the $\delta^{18}O$ and $\delta^{13}C$ values of fluids which were fully equilibrated with carbonates at different temperatures under the conditions with high enough W/R. To match up with both the $\delta^{18}O$ and $\delta^{13}C$ ratios of sample LD006, the most likely fluids were meteoric because its $\delta^{18}O$ value is usually <0% and the $\delta^{13}C$ value of its dissolved CO_2 is around −8‰ (Schidlowski, 2001), and the most realistic temperature is between 75 and 100 °C. Therefore, compared to other magnesite samples, the $\delta^{13}C$ decrease and the $\delta^{18}O$ increase of sample LD006 resulted from post-metamorphic interaction between the massive magnesite and meteoric water at temperature of 75−100 °C.

6. CONCLUSIONS

(1) The Dashiqiao magnesite belt is the largest $MgCO_3$ producer in the world, with magnesite ores being hosted in the 2.2−2.174 Ga Dashiqiao Formation, Liaohe Group, in the northeastern North China Craton. Magnesite samples from the orebody yield $\delta^{13}C$ ratios of 0.1−0.9‰ with an average of 0.4 ± 0.2‰ ($n = 12$), and $\delta^{18}O$ value of 9.2−16.9‰ with an average of 13.3 ± 2.5‰ ($n = 14$). Six dolomitic marble samples from the footwall yield $\delta^{13}C$ and $\delta^{18}O$ values of 0.6−1.4‰ and 16.4−19.5‰, with averages of 1.2 ± 0.3‰ and 18.2 ± 1.1‰, respectively. These data clearly exhibit positive $\delta^{13}C$ anomalies.

(2) It is estimated that the primary sediments of the Dashiqiao Formation might possess $\delta^{13}C$ values of >4.2‰, and $\delta^{18}O$ values of >21.5‰. The Palaeoproterozoic carbonate strata in the Jiao-Liao-Ji Belt, North China Craton, therefore records the global GOE.

(3) The carbonate rocks in the Dashiqiao magnesite belt reduced the $\delta^{13}C$ and $\delta^{18}O$ values during post-depositional geological modifications, as indicated by the much lower and variable $\delta^{18}O$ ratios relative to global carbonates, and the negative $\delta^{13}C$ values in talc-bearing dolomite and veinlet-filled magnesite samples.

(4) The post-depositional geological processes were complex, including diagenesis–metamorphism and associated hydrothermal alteration, limited post-metamorphic faulting, and then local low-temperature fluid–rock interaction. These, in addition to the Palaeoproterozoic evaporate sedimentation in a high-Mg lagoon, might have favoured the formation of the giant Dashiqiao magnesite belt. Thus, the formation of the Dashiqiao magnesite belt records a multistage and polygenetic history.

Table 5. The calculated $\delta^{13}C$ and $\delta^{18}O$ values of fluids equilibrated to the veinlet-filled magnesite at different temperatures

	Reaction temperature					
	25 °C	50 °C	75 °C	100 °C	125 °C	150 °C
$\delta^{13}C_{CO2}$	−15.4	−12.3	−9.7	−7.7	−6.1	−4.8
$\delta^{18}O_{H2O}$	−15	−9.9	−5.8	−2.5	0.1	2.4

ACKNOWLEDGEMENTS

This study was granted by the National 973-Program (project nos. 2012CB416602, 2006CB403508), the National Natural Science Foundation of China (nos. 40352003, 40425006, 40373007) as well as Frontier Field Project of the State Key Laboratory of Ore Deposit Geochemistry, Institute of Geochemistry, Chinese Academy of Sciences, Guiyang. Prof. Zhitong Li (Shenyang) and Senior Engineers Wei He, Yongfeng Qu and Youguang Jing helped field investigations. The authors sincerely thank Professors Shaoyong Jiang and Hongfei Ling for valuable comments which greatly helped in improving an earlier version of the paper. Constructive suggestions, pertinent comments and careful corrections by Professors F. Pirajno, M.G. Zhai and Ian D. Somerville greatly improved the quality of the manuscript.

REFERENCES

Aharon, P. 2005. Redox stratification and anoxia of the early Precambrian oceans: implications for carbon isotope excursions and oxidation events. *Precambrian Research* **137**, 207–222.

Anbar, A.D., Duan, Y., Lyons, T.W., Arnold, G.L., Kendall, B., Creaser, R.A., Kaufman, A.J., Gordon, G.W., Scott, C., Garvin, J., Buick, R. 2007. A whiff of oxygen before the Great Oxidation Event? *Science* **317**, 1903–1906.

Baker, A.J., Fallick, A.E. 1989a. Evidence from Lewisian limestone for isotopically heavy carbon in two-thousand-million-year-old sea water. *Nature* **337**, 352–354.

Baker, A.J., Fallick, A.E. 1989b. Heavy carbon in two-billion-year-old marbles from Lofoten–Vesteralen, Norway: implications for the Precambrian carbon cycle. *Geochimica et Cosmochimica Acta* **53**, 1111–1115.

Banner, J.L. 2004. Radiogenic isotopes: systematics and applications to earth surface processes and chemical stratigraphy. *Earth-Science Reviews* **65**, 141–194.

Banner, J.L., Hanson, G.N. 1990. Calculation of simultaneous isotopic and trace element variations during water–rock interaction with applications to carbonate diagenesis. *Geochimica et Cosmochimica Acta* **54**, 3123–3137.

Bekker, A., Eriksson, K.A. 2003. A Paleoproterozoic drowned carbonate platform on the southeastern margin of the Wyoming Craton: a record of the Kenorland breakup. *Precambrian Research* **120**, 327–364.

Bekker, A. Kaufman, A.J. 2007. Oxidative forcing of global climate change: a biogeochemical record across the oldest Paleoproterozoic ice age in North America. *Earth and Planetary Science Letters* **258**, 486–499.

Bekker, A., Karhu, J.A., Kaufman, A.J. 2006. Carbon isotope record for the onset of the Lomagundi carbon isotope excursion in the Great Lakes area, North America. *Precambrian Research* **148**, 145–180.

Bekker, A., Karhu, J.A., Eriksson, K.A., Kaufman, A.J. 2003a. Chemostratigraphy of Palaeoproterozoic carbonate successions of the Wyoming Craton: tectonic forcing of biogeochemical change? *Precambrian Research* **120**, 279–325.

Bekker, A., Kaufman, A.J., Karhu, J.A., Eriksson, K.A. 2005. Evidence for Paleoproterozoic cap carbonates in North America. *Precambrian Research* **137**, 167–206.

Bekker, A., Kaufman, A.J., Karhu, J.A., Beukes, N.J., Swart, Q.D., Coetzee, L.L., Eriksson, K.A. 2001. Chemostratigraphy of the Paleoproterozoic Duitschland Formation, South Africa: implications for coupled climate change and carbon cycling. *American Journal of Science* **301**, 261–285.

Bekker, A., Sial, A.N., Karhu, J.A., Ferrerira, V.P., Noce, C.M., Kaufman, A.J., Romano, A.W., Pimentel, M.M. 2003b. Chemostratigraphy of carbonates from the Minas Supergroup, Quadrilátero Ferrífero (Iron Quadrangle), Brazil: a stratigraphic record of early Proterozoic atmospheric, biogeochemical and climatic change. *American Journal of Science* **303**, 865–904.

Bottinga, Y. 1969. Calculated fractionation factors for carbon and hydrogen isotope exchange in the system calcite–carbon dioxide–graphite–methane–hydrogen–water vapour. *Geochimica et Cosmochimica Acta* **33**, 49–64.

Buick, I.S., Uken, R., Gibson, R.L., Wallmach, T., 1998. High $\delta^{13}C$ Paleoproterozoic carbonates from the Transvaal Supergroup, South Africa. *Geology* **26**, 875–878.

Chen, C.X., Cai, K.Q. 2000. Minerogenic system of magnesian nonmetallic deposits in Early Proterozoic Mg-rich carbonate formations in eastern Liaoning Province. *Acta Geologica Sinica* **74**, 623–631.

Chen, C.X., Jiang, S.Y., Cai, K.Q., Ma, B. 2003a. Metallogenic conditions of magnesite and talc deposits in early Proterozoic Mg-rich carbonate formations, eastern Liaoning province. *Mineral Deposits* **22**(2), 166–176 (in Chinese with English abstract).

Chen, C.X., Ni, P., Cai, K.Q., Zhai, Y.S., Deng, J. 2003b. The minerogenic fluids of magnesite and talc deposits in the Paleoproterozoic Mg-rich carbonate formations in eastern Liaoning Province. *Geological Review* **49**(6), 646–651 (in Chinese with English abstract).

Chen, Y.J. 1988. Catastrophe of the geologic environment at 2300 Ma. Abstracts of International Symposium on Geochemistry and Mineralization of Proterozoic Mobile Belts, 6–10 September, Tianjin, 11

Chen, Y.J. 1990. Evidences for the catastrophe in geologic environment at about 2300 Ma and the discussions on several problems. *Journal of Stratigraphy* **14**, 178–186 (in Chinese with English abstract).

Chen, Y.J., Fu, S.G. 1992. *Gold Mineralization in West Henan, China*. Chinese Seismological Press: Beijing, 234 pp (in Chinese with English abstract).

Chen, Y.J., Su, S.G. 1998. Catastrophe in geological environment at 2300 Ma. *Mineralogical Magazine* **62A**(1), 320–321.

Chen, Y.J., Zhao, Y.C. 1997. Geochemical characteristics and evolution of REE in the Early Precambrian sediments: evidences from the southern margin of the North China craton. *Episodes* **20**, 109–116.

Chen, Y.J., Hu, S.X., Lu, B. 1998. Contrasting REE geochemical features between Archean and Proterozoic khondalite series in North China Craton. *Mineralogical Magazine* **62A**(1), 318–319.

Chen, Y.J., Liu, C.Q., Chen, H.Y., Zhang, Z.J., Li, C. 2000. Carbon isotope geochemistry of graphite deposits and ore-bearing khondalite series in North China: implications for several geoscientific problems. *Acta Petrologica Sinica* **16**, 233–244 (in Chinese with English abstract).

Chen, Y.J., Ouyang, Z.Y., Yang, Q.J., Deng, J. 1994. A new understanding of the Archean–Proterozoic boundary. *Geologic Review* **40**, 483–488 (in Chinese with English abstract).

Chen, Y.Q., Jiang, S.Y., Ling, H.F., Pan, J.Y., Lai, M.Y. 2005. Oxygen isotope calibration of carbonate minerals measured by Finnigan MAT-252 gas mass spectrometer. *Journal of Chinese Mass Spectrometry Society* **26**(2), 115–118 (in Chinese with English abstract).

Derry, L.A., Kaufman, A.J., Jacobsen, S.B. 1992. Sedimentary cycling and environmental changes in the Late Proterozoic: evidence from stable and radiogenic isotopes. *Geochimica et Cosmochimica Acta* **56**, 1317–1329.

Diwu, C., Sun, Y., Guo, A., Wang, H., Liu, X. 2011. Crustal growth in the North China Craton at ~2.5 Ga: evidence from in situ zircon U–Pb ages, Hf isotopes and whole-rock geochemistry of the Dengfeng complex. *Gondwana Research* **20**, 149–170.

Dong, Q.S., Feng, B.Z., Li, X.J. 1996. The lithofacies and palaeogeographical setting of Haicheng–Dashiqiao superlarge magnesite deposits, Liaoning province. *Journal of Changcun University Earth Science* **26** (Supp.), 69–73.

EI Tabakh, M., Grey, K., Pirajno, F., Schreiber, B.C. 1999. Pseudomorphs after evaporitic minerals interbedded with 2.2 Ga stromatolites of the Yirrada basin, Western Australia. *Geology* **27**, 871–874.

Faure, M., Lin, W., Monie, P., Bruguier, O. 2004. Palaeoproterozoic arc magmatism and collision in Liaodong Peninsula (north-east China). *Terra Nova* **16**, 75–80.

Feng, W.M., Zheng, Y.F., Zhou, J.B. 2003. Carbon and oxygen isotope Geochemistry of marbles from the Dabie-Sulu orogenic belt. *Acta Petrologica Sinica* **19**, 468–478 (in Chinese with English abstract).

Friedman, I., O'Neil, J.R. 1977. Compilation of stable isotope fractionation factors of geochemical interest. In: *Data of Geochemistry*, 6th edn., Fleischer M. (ed.). *United States Geological Survey Professional Paper* 440-KK. U.S.Geological Survey: Washington, D.C., 49.

Gauthier-Lafaye, F., Weber, F. 1989. The Francevillian (Lower Proterozoic) uranium ore deposits of Gabon. *Economic Geology* **84**, 2267–2285.

Guerrera, A., Peacock, S.M., Knauth, L.P. 1997. Large ^{18}O and ^{13}C depletion in greenschist facies carbonate rocks, Western Arizona. *Geology* **25**, 943–946.

He, G.P., Ye, H.W. 1998. Two type of early Proterozoic metamorphism in the eastern Liaoning to southern Jilin and their tectonic implication. *Acta Petrologica Sinica* **14**, 152–162 (in Chinese with English abstract).

Hoefs, J. 1997. *Stable Isotope Geochemistry (4th edition)*. Springer-Verlag: Berlin.

Huston, D.L., Logan, G.A. 2004. Barite, BIFs and bugs: evidence for the evolution of the Earth's early atmosphere. *Earth and Planetary Science Letters* **220**, 41–55.

Jacobsen, S.B., Kaufman, A.J. 1999. The Sr, C and O isotopic evolution of Neoproterozoic seawater. *Chemical Geology* **161**, 37–57.

Jiang, C.C. 1987. *The Early Precambrian Geology of Eastern Liaoning Province and Jilin Province*. Liaoning Science and Technology Publishing House: Shenyang (in Chinese).

Jiang, S.Y., Chen, C.X., Chen, Y.Q., Jiang, Y.H., Dai, B.Z., Ni, P. 2004. Geochemistry and genetic model for the giant magnesite deposits in the eastern Liaoning province, China. *Acta Petrologica Sinica* **20**, 765–772 (in English with Chinese abstract).

Jiang, S.Y., Palmer, M.R., Peng, Q.M., Yang, J.H. 1997. Chemical and stable isotopic compositions of Proterozoic metamorphosed evaporites and associated tourmalines from the Houxianyu borate deposit, eastern Liaoning, China. *Chemical Geology* **135**, 189–211.

Karhu, J.A. 1993. Palaeoproterozoic evolution of the carbon isotope ratios of sedimentary carbonates in the Fennoscandian Shield. *Geological Survey of Finland Bulletin* **371**, 87.

Karhu, J.A., Holland, H.D. 1996. Carbon isotopes and the rise of atmospheric oxygen. *Geology* **24**, 867–870.

Konhauser, K.O., Pecoits, E., Lalonde, S.V., Papineau, D., Nisbet, E.G., Barley, M.E., Arndt, N.T., Zahnle, K., Kamber, B.S. 2009. Oceanic nickel depletion and a methanogen famine before the Great Oxidation Event. *Nature* **458**, 750–753.

Kusky, T.M. 2011. Geophysical and geological tests of tectonic models of the North China Craton. *Gondwana Research* **20**, 26–35.

Li, S.Z., Zhao, G.C. 2007. SHRIMP U–Pb zircon geochronology of the Liaoji granitoids: constraints on the evolution of the Paleoproterozoic Jiao-Liao-Ji belt in the Eastern Block of the North China Craton. *Precambrian Research* **158**, 1–16.

Li, S.Z., Zhao, G.C., Sun, M., Han, Z.Z., Luo, Y., Hao, D.F., Xia, X.P. 2005. Deformation history of the Paleoproterozoic Liaohe assemblage in the eastern block of the North China Craton. *Journal of Asian Earth Sciences* **24**, 659–674.

Li, S.Z., Zhao, G.C., Sun, M., Han, Z.Z., Zhao, G.T., Hao, D.F. 2006. Are the South and North Liaohe Groups of the North China Craton different exotic terranes? Nd isotope constraints. *Gondwana Research* **9**, 198–208.

Liaoning Bureau of Geology and Mineral Resources. **1989**. *The Regional Geology of Liaoning Province*. Geological Publishing House: Beijing (in Chinese with English abstract).

Liu, S.W., Santosh, M., Wang, W., Bai, X., Yang, P. 2011. Zircon U–Pb chronology of the Jianping Complex: implications for the Precambrian crustal evolution history of the northern margin of the North China Craton. *Gondwana Research* **20**, 48–63.

Liu, P., Liu, F., Yang, H., Wang, F., Liu, J. 2012. Protolith ages and timing of peak and retrograde metamorphism of the high-pressure granulites in the Shandong Peninsula, eastern North China Craton. *Geoscience Frontiers* **3**, 923–943.

Lu, X.P., Wu, F.Y., Lin, J.Q., Sun, D.Y., Zhang, Y.B., Guo, C.L. 2004. Geochronological successions of the Early Precambrian granitic magmatism in southern Liaoning Peninsula and its constraints on tectonic evolution of the North China Craton. *Chinese Journal of Geology* **39**, 123–138 (in Chinese with English abstract).

Lu, X.P., Wu, F.Y., Guo, J.H., Wilde, S.A., Yang, J.H., Liu, X.M., Zhang, X.O. 2006. Zircon U–Pb geochronological constraints on the Paleoproterozoic crustal evolution of the Eastern Block in the North China Craton. *Precambrian Research* **146**, 138–164.

Luo, Y., Sun, M., Zhao, G.C., Ayers, J.C., Li, S.Z., Xia, X.P., Zhang, J. H. 2008. A comparison of U–Pb and Hf isotopic compositions of detrital zircons from the North and South Liaohe Group: constraints on the evolution of the Jiao-Liao-Ji Belt, North China Craton. *Precambrian Research* **163**, 279–306.

Luo, Y., Sun, M., Zhao, G.C., Li, S.Z., Xu, P., Ye, K., Xia, X.P. 2004. LA ICP-MS U−Pb zircon ages of the Liaohe Group in the Eastern Block of the North China Craton: constraints on the evolution of the Jiao-Liao-Ji Belt. *Precambrian Research* **134**, 349–371.

Maheshwari, A., Sial, A.N., Gaucher, C., Bossi, J., Bekker, A., Ferreira, V.P., Romano, A.W. 2010. Global nature of the Paleoproterozoic Lomagundi carbon isotope excursion: a review of occurrences in Brazil, India, and Uruguay. *Precambrian Research* **182**, 274–299.

Matthews, A., Katz, A. 1977. Oxygen isotope fractionation during the dolomitisation of calcium carbonate. *Geochimica et Cosmochimica Acta* **41**, 1431–1438.

Melezhik, V.A., Fallick, A.E. 1996. A widespread positive $\delta^{13}C_{carb}$ anomaly at 2.33–2.06 Ga on the Fennoscandian Shield: a paradox? *Terra Nova* **8**, 141–157.

Melezhik, V.A., Bingen, B., Fallick, A.E., Gorokhov, I.M., Kuznetsov, A.B., Sandstad, J.S., Solli, A., Bjerkgård, T., Henderson, I., Boyda, R., Jamal, D., Monize, A. 2008. Isotope chemostratigraphy of marbles in northeastern Mozambique: apparent depositional ages and tectonostratigraphic implications. *Precambrian Research* **162**, 540–558.

Melezhik, V.A., Fallick, A.E., Pokrovsky, B.G. 2005a. Enigmatic nature of thick sedimentary carbonates depleted in ^{13}C beyond the canonical mantle value: the challenges to our understanding of the terrestrial carbon cycle. *Precambrian Research* **137**, 131–165.

Melezhik, V.A., Fallick, A.E., Clark, A. 1997. Two billion year old isotopically heavy carbon: evidence from the Labrador Trough, Canada. *Canadian Journal of Earth Sciences* **34**, 271–285.

Melezhik, V.A., Fallick, A.E., Medvedev, P.V., Makarikhin, V.V. 1999. Extreme $^{13}C_{carb}$ enrichment in *ca*. 2.0 Ga magnesite–stromatolite–dolomite–'red beds' association in a global context: a case for the worldwide signal enhanced by a local environment. *Earth-Science Reviews* **48**, 71–120.

Melezhik, V.A., Gorokhov, I.M., Fallick, A.E., Gjelle, S. 2001a. Strontium and carbon isotope geochemistry applied to dating of carbonate sedimentation: an example from high-grade rocks of the Norwegian Caledonides. *Precambrian Research* **108**, 267–292.

Melezhik, V.A., Gorokhov, I.M., Kuznetsov, A.B., Fallick, A.E. 2001b. Review article: chemostratigraphy of Neoproterozoic carbonates: implications for 'blind dating'. *Terra Nova* **13**, 1–11.

Melezhik, V.A., Kuznetsov, A.B., Fallick, A.F., Smith, R.A., Gorokhov, I.M., Jamal, D., Catuane, F. 2006. Depositional environments and an apparent age for the Geci meta-limestones: constraints on the geological history of northern Mozambique. *Precambrian Research* **148**, 19–31.

Melezhik, V.A., Roberts, D., Fallick, A.E., Gorokhov, I.M., Kuznetsov, A.B. 2005b. Geochemical preservation potential of high-grade calcite marble versus dolomite marble: implication for isotope chemostratigraphy. *Chemical Geology* **216**, 203–224.

Peng, Q.M. 2002. The Paleoproterozoic Mg–Fe borate deposits of Liaoning and Jilin Provinces, Northeast China. *Economic Geology* **97**, 93–108.

Peng, Q.M., Palmer, M.R. 1995. The Paleoproterozoic boron deposits in eastern Liaoning, China: a metamorphosed evaporite. *Precambrian Research* **72**, 185–197.

Purohit, R., Sanyal, P., Roy, A.B., Bhattacharya, S.K. 2010. ^{13}C enrichment in the Palaeoproterozoic carbonate rocks of the Aravalli Supergroup, northwest India: influence of depositional environment. *Gondwana Research* **18**, 538–546.

Qi, J.P., Zhang, J., Tang, G.J. 2005. Carbon and oxygen isotope composition of the Meso-Neoproterozoic strata south of the Xiong'er Terrane: evidences of the CMF model. *Acta Petrologica Sinica* **21**, 1365–1372 (in Chinese with English abstract).

Ray, J.S., Veizer, J., Davis, W.J. 2003. C, O, Sr and Pb isotope systematics of carbonate sequences of the Vindhyan Supergroup, India: age, diagenesis, correlations and implications for global events. *Precambrian Research* **121**, 103–140.

Rosenbaum, J., Sheppard, S.M.F. 1986. An isotopic study of siderites, dolomites and ankerites at high temperatures. *Geochimica et Cosmochimica Acta* **50**, 1147–1150.

Santosh, M. 2010. Assembling North China Craton within the Columbia supercontinent: the role of double-sided subduction. *Precambrian Research* **178**, 149–167.

Santosh, M., Liu, S.J., Tsunogae, T., Li, J.H. 2012. Paleoproterozoic ultrahigh-temperature granulites in the North China Craton: implications for tectonic models on extreme crustal metamorphism. *Precambrian Research* **222–223**, 77–106.

Schidlowski, M. 1988. A 3800-million-year isotopic record of life from carbon in sedimentary rocks. *Nature* **333**, 313–318.

Schidlowski, M., 2001. Carbon isotopes as biogeochemical recorders of life over 3.8 Ga of Earth history: evolution of a concept. *Precambrian Research* **106**, 117–134.

Schidlowski, M., Eichmann, R., Junge, C.E. 1975. Precambrian sedimentary carbonates: carbon and oxygen isotope geochemistry and implications for the terrestrial oxygen budget. *Precambrian Research* **2**, 1–69.

Schidlowski, M., Eichmann, R., Junge, C.E. 1976. Carbon isotope geochemistry of the Precambrian Lomagundi carbonate province, Rhodesia. *Geochimica et Cosmochimica Acta* **40**, 449–455.

Sheppard, S.M.F., Schwarcz, H.P. 1970. Fractionation of carbon and oxygen isotopes and magnesium between coexisting metamorphic calcite and dolomite. *Contributions to Mineralogy and Petrology* **26**, 161–198.

Shieh, Y.N., Taylor, H.P., Jr. 1969. O and C isotope studies of contact metamorphism of carbonate rocks. *Journal of Petrology* **10**, 307–331.

Sreenivas, B., Sharma, D.S., Kumar, B., Patil, D.J., Roy, A.B., Srinivasan, R. 2001. Positive $\delta^{13}C$ excursion in carbonate and organic fractions from the Paleoproterozoic Aravalli Supergroup, Northwestern India. *Precambrian Research* **106**, 277–290.

Sun, M., Armstrong, R.L., Lambert, R.S., Jiang, C.C., Wu, J.H. 1993. Petrochemistry and Sr, Pb and Nd isotopic geochemistry of Paleoproterozoic Kuandian Complex, the eastern Liaoning Province, China. *Precambrian Research* **62**, 171–190.

Tam, P.Y., Zhao, G.C., Liu, F., Zhou, X., Sun, M., Li, S.Z. 2011. Timing of metamorphism in the Paleoproterozoic Jiao-Liao-Ji Belt: new SHRIMP U–Pb zircon dating of granulites, gneisses and marbles of the Jiaobei massif in the North China Craton. *Gondwana Research* **19**, 150–162.

Tam, P.Y., Zhao, G.C., Zhou, X., Sun, M., Guo, J., Li, S., Yin, C., Wu, M., He, Y. 2012. Metamorphic P–T path and implications of high-pressure pelitic granulites from the Jiaobei massif in the Jiao-Liao-Ji Belt, North China Craton. *Gondwana Research* **22**, 104–117.

Tang, H.S., Chen, Y.J. Wu, G., Lai, Y. 2011. Paleoproterozoic positive $\delta^{13}C_{carb}$ excursion in northeastern Sino-Korean craton: evidence of the Lomagundi Event. *Gondwana Research* **19**, 471–481.

Tang, H.S., Chen, Y.J., Santosh, M., Zhong, H., Yang, T. 2012. REE geochemistry of carbonates from the Guanmenshan Formation, Liaohe Group, NE Sino-Korean Craton: implications for seawater compositional change during the Great Oxidation Event. *Precambrian Research* doi: 10.1016/j.precamres.2012.02.005

Tang, H.S., Chen, Y.J., Wu, G., Yang, T. 2009. Rare earth element geochemistry of carbonates of Dashiqiao Formation, Liaohe Group, eastern Liaoning province: implications for Lomagundi Event. *Acta Petrologica Sinica* **25**, 3075–3093 (in Chinese with English abstract).

The Ministry of Land and Resources P.R.C. 2001. *Reporting the Land and Resources of China in 2000*. Geological Publishing House: Beijing (in Chinese).

Tikhomirova, M., Makarakhin, V.V. 1993. Possible reasons for the $\delta^{13}C$ anomaly of the Lower Proterozoic sedimentary carbonates. *Terra Nova* **5**, 244–248.

Tsunogase, T., Liu, S.J., Santosh, M., Shimizu, H., Li, J.H. 2011. Ultrahigh-temperature metamorphism in Daqingshan, Inner Mongolia Suture Zone, North China Craton. *Gondwana Research* **20**, 36–47.

Tu, G.C. 1996. The discussion on some CO_2 problems. *Earth Science Frontiers* **3**(3), 53–62 (in Chinese with English abstract).

Tu, G.C., Zhao, Z.H., Qiu, Y.Z. 1985. Evolution of Precambrian REE mineralization. *Precambrian Research* **27**, 131–151.

Valley, J.M. 1986. Stable isotope geochemistry of metamorphic rocks. *Reviews in Mineralogy* **16**, 445–489.

Veizer, J., Hoefs, J. 1976. The nature of $^{18}O/^{16}O$ and $^{13}C/^{12}C$ secular trends in sedimentary carbonate rocks. *Geochimica et Cosmochimica Acta* **40**, 1387–1395.

Veizer, J., Ala, D., Azmy, K., Bruckschen, P., Buhl, D., Bruhn, F., Carden, G.A.F., Diener, A., Ebneth, S., Godderis, Y., Jasper, T., Korte, C., Pawallek, F., Podlaha, O.G., Strauss, H. 1999. $^{87}Sr/^{86}Sr$, $\delta^{13}C$ and $\delta^{18}O$ evolution of Phanerozoic seawater. *Chemical Geology* **161**, 59–88.

Veizer, J., Clayton, R.N., Hinton, R.W. 1992. Geochemistry of Precambrian carbonates: IV. Early Paleoproterozoic (2.25 ± 0.25 Ga) seawater. *Geochimica et Cosmochimica Acta* **56**, 875–885.

Wada, H., Suzuki, K. 1983. Carbon isotopic thermometry calibrated by dolomite-calcite solvus temperatures. *Geochimica et Cosmochimica Acta* **47**, 697–706.

Walravan, F., Armstrong, R.A., Kruger, F.J. 1990. A chronostratigraphic framework for the north-central Kaapvaal craton, the Bushveld Complex and the Vredefort structure. *Tectonophysics* **171**, 23–48.

Wan, Y.S., Song, B., Liu, D.Y., Wilde, S.A., Wu, J.S., Shi, Y.R., Yin, X. Y., Zhou, H.Y. 2006. SHRIMP U–Pb zircon geochronology of Palaeoproterozoic metasedimentary rocks in the North China Craton: evidence for a major Late Palaeoproterozoic tectonothermal event. *Precambrian Research* **149**, 249–271.

Wan, Y.S., Liu, D.Y., Wang, W., Song, T., Kröner, A., Dong, C., Zhou, H., Yin, X.Y. 2011. Provenance of Meso- to Neoproterozoic cover sediments at the Ming Tombs, Beijing, North China Craton: an integrated study of U–Pb dating and Hf isotopic measurement of detrital zircons and whole-rock geochemistry. *Gondwana Research* **20**, 219–242.

Wang, A.J., Peng, Q.M., Palmer, M.R. 1998. Salt-dome-controlled precipitation of Paleoproterozoic Fe–Cu sulfide deposits, eastern Liaoning, Northeastern China. *Economic Geology* **93**, 1–14.

Wang, H.Y., Peng, X.L. 2008. Genesis of magnetite of the Wengquangou vonsenite deposit, Fengcheng county, Liaoning Province. *Geology in China* **35**, 1299–1306.

Xiao, R.G., Takao, O., Fei, H.C., Nomura, M. 2003. Sedimentary–metamorphic boron deposits and their boron isotopic compositions in eastern Liaoning Province. *Geoscience* **17**, 137–142 (in Chinese with English abstract).

Young, G.M. 2012a. Precambrian supercontinents, glaciations, atmospheric oxygenation, metazoan evolution and an impact that may have changed the second half of Earth history. *Geoscience Frontiers*, http://dx.doi.org/10.1016/j.gsf.2012.07.003.

Young, G.M., 2012b. Secular changes at the Earth's surface: evidence from palaeosols, some sedimentary rocks, and palaeoclimatic perturbations of the Proterozoic Eon. *Gondwana Research*, 10.1016/j.gr.2012.07.016.

Zhai, M.G., Peng, P. 2007. Paleoproterozoic events in the North China Craton. *Acta Petrologica Sinica* **23**, 2665–2682 (in Chinese with English abstract).

Zhai, M.G., Santosh, M. 2011. The Early Precambrian odyssey of the North China Craton: a synoptic overview. *Gondwana Research* **20**, 6–25.

Zhai, M.G., Li, T.S., Peng, P., Hu, B., Liu, F., Zhang, Y.B., Guo, J.H. 2010. Precambrian key tectonic events and evolution of the North China Craton. In: *The Evolving Continents: Understanding Processes of Continental Growth*, Kusky T.M., Zhai M.-G., Xiao W.-J. (eds). Geological Society of London, Special Publication, London **338**, 235–262.

Zhao, G.C., Sun, M., Wilde, S.A. Li, S.H. 2004. A Paleo-Mesoproterozoic supercontinent: assembly, growth and breakup. *Earth-Science Reviews* **67**, 91–123.

Zhao, G.C., Sun, M., Wilde, S.A. Li, S.Z. 2005. Late Archean to Paleoproterozoic evolution of the North China Craton: key issues revisited. *Precambrian Research* **136**, 177–202.

Zhao, Z.H. 2010. Banded iron formation and great oxidation event. *Earth Science Frontiers* **17**, 1–12 (in Chinese with English abstract).

Zhang, Q.S., Yang, Z.S., Wang, Y.J. 1988. *Early Crust and Mineral Deposits of Liaodong Peninsula*. Geological Publishing House: Beijing (in Chinese).

Zheng, Y.F., Xiao, W.J., Zhao, G.C. 2012. Introduction to tectonics of China. *Gondwana Research*, 10.1016/j.gr.2012.10.001.

